BSGF - Earth Sciences Bulletin 2026, 197, 11
© P. Gatt Published by EDP Sciences 2026
https://doi.org/10.1051/bsgf/2026002

BSGF Earth Sciences Bulletin
Available online at:
www.bsgf.fr

Recent evolution of the Mediterranean realm: Exploring the links between deep and shallow processes in a plate convergent setting Christian Gorini, Anouk Beniest, Andréa Billi, Nicolas Chamot-Rooke, Jacques Déverchère and Juan I. Soto (Guest editors)

Neotectonic shortening and foreland structural evolution of the Malta Horst Cenozoic carbonate succession, Central Mediterranean

Peter Gatt*

Malta College of Arts, Science and Technology, Paola, Malta

Received: 23 May 2025 / Accepted: 1 February 2026 / Publishing online: 1 May 2026

Abstract – The Malta Horst is a NW–SE-trending, 30 km wide structural high situated on the southern Hyblean-Malta Plateau, which is an African continental indenter in collision with Eurasia. Sediments consist of a shallow marine carbonate platform succession (Mesozoic to Oligocene) capped by Miocene pelagic carbonates and marl. Utilizing seismic profiles, well data, and outcrop observations, this study provides the first description of kilometer-scale contractional structures within the horst and analyzes the reactivation of normal faults by transcurrent movement under NW compression. The tectonic evolution of this foreland region is defined by five distinct phases (A through E), alternating between extension and compression. This cyclicity reflects the interplay between the migrating Calabrian Arc and the converging African craton. Initial NE–SW trending faults (Phases A and B) developed during the Late Oligocene to Early Miocene, coinciding with platform drowning. Following Tortonian uplift (Phase C), accelerated migration of the Calabrian arc during Phase D triggered N–S extension, establishing the NW–SE and NE–SW normal faults that bound the Malta Horst. The neotectonic regime (Phase E) marks a return to dominance of the NW-directed compression by the African craton as the Calabrian Arc migration decelerated. This regional stress field has reactivated the NW–SE marginal normal faults through strike-slip motion. The combination of transcurrent drag and regional compression has inverted Phase A NE–SW normal faults into oblique reverse faults. These thrusts sole along a weak top Eocene evaporite décollement, producing a series of folds and inverted basins within 10 km of the horst's northeast margin. Onshore, these structures are manifest as en echelon, non-cylindrical, and doubly plunging folds that define the topography of Malta's northeast coast. These shear zone structures are thin-skinned deformations in Oligo-Miocene sediments controlled by thick-skinned, W–E transcurrent movement in the crust and Mesozoic sediments. Ongoing compression suggests an increase in seismic risk proximal to the Maltese Islands, with significant implications for local geohazard frequency and magnitude.

Keywords: Maltese islands / foreland / inversion tectonics / foreland / carbonate platforms

Résumé – Raccourcissement néotectonique et évolution structurale de l'avant-pays de la série carbonatée cénozoïque du horst de Malte, Méditerranée centrale. Le Horst de Malte est un haut-fond structural de 30 km de large, orienté NO-SE, situé sur la partie sud du plateau Hybléen-Maltais, qui constitue un poinçon continental africain en collision avec l'Eurasie. La sédimentation se compose d'une succession de plateforme carbonatée marine peu profonde (du Mésozoïque à l'Oligocène), surmontée par des carbonates pélagiques et des marnes du Miocène. En s'appuyant sur des profils sismiques, des données de puits et des observations d'affleurements, cette étude fournit la première description de structures de contraction à l'échelle kilométrique au sein du horst et analyse la réactivation de failles normales par un mouvement transcurrent sous une compression NO. L'évolution tectonique de cette région d'avant-pays est définie par cinq phases distinctes (A à E), alternant entre extension et compression. Cette cyclicité reflète l'interaction entre la migration de l'arc calabrais et la convergence du craton africain: Phases A et B (Oligocène supérieur à Miocène inférieur); Développement des premières failles orientées NE-SO, coïncidant avec l'ennoiement de la plateforme; Phase C (Tortonien), soulèvement tectonique; Phase D, l'accélération de la migration de l'arc calabrais déclenche une extension N–S, établissant les failles normales NO-SE et NE-SO qui délimitent le horst de Malte et, Phase E, (régime néotectonique) marque le retour à la dominance de la compression

*Corresponding author: pgatt.geo@gmail.com

dirigée vers le NO par le craton africain, alors que la migration de l'arc calabrais ralentit. Ce champ de contraintes régional a réactivé les failles normales marginales NO-SE par un mouvement de décrochement. La combinaison de l'entraînement transcurrent et de la compression régionale a inversé les failles normales NE-SO de la Phase A en failles inverses obliques. Ces chevauchements s'enracinent le long d'un niveau de décollement ductile d'évaporites du sommet de l'Éocène, produisant une série de plis et de bassins inversés à moins de 10 km de la marge nord-est du horst. À terre, ces structures se manifestent par des plis en échelon, non cylindriques et à double plongement, qui définissent la topographie de la côte nord-est de Malte. Ces structures de zone de cisaillement sont des déformations de couverture (*thin-skinned*) dans les sédiments oligo-miocènes, contrôlées par un mouvement transcurrent E-O de socle (*thick-skinned*) dans la croûte et les sédiments mésozoïques. La compression actuelle suggère une augmentation du risque sismique à proximité des îles maltaises, avec des implications significatives pour la fréquence et l'ampleur des risques géologiques locaux.

Mots-clés : Îles maltaises / avant-pays / plissement en échelon / anticlinaux / plates-formes carbonatées

1 Introduction

The Late Cretaceous convergence of the African and Eurasian plates triggered the development of several Mediterranean orogenic belts (Dewey *et al.*, 1973; Rosenbaum and Lister, 2004; van Hinsbergen *et al.*, 2020a). The orogenic loading and migrating arcs have downflexed the African foreland, with thick-skinned tectonics (Morticelli *et al.*, 2015) generating foreland extension perpendicular to the foredeep (Decelles and Giles, 1996). In the Central Mediterranean, the Pelagian Block has been loaded by the Sicilian-Maghrebian orogenic belt (Argnani, 1987; Butler *et al.*, 1992; Corti *et al.*, 2006; Maiorana *et al.*, 2023). Crustal inhomogeneity of the Pelagian foreland along the collisional front resulted in its segmentation into three distinct blocks separated by N–S trending strike-slip faults (Ben-Avraham *et al.*, 1995):

1 The Hyblean-Malta Plateau (HMP): A trapezoidal-shaped, African continental indenter bounded by three transcurrent faults: the Scicli Fault on the west, the Malta Escarpment Fault on the east, and the Medina Wrench on the south (S1, S2, and S3 in Fig. 1a). Owing to its relative thickness and buoyancy, the rigid crust resisted significant subduction along the SE Sicilian collision front (Cowie and Kusznir, 2012; Gardiner *et al.*, 1995), leading to the formation of oroclines along its margins (Ben-Avraham *et al.*, 1995; Rosenbaum, 2014).
2 The Gela Basin: Situated to the west of the HMP, this downflexed basin is further delimited in the western Sicily Channel by the seismically active Sciacca strike-slip fault (Civile *et al.*, 2021; Soumaya *et al.*, 2015).
3 The Ionian Block: lies to the east of the HMP, divided by the Malta Escarpment transform fault. Characterized by oceanic crust at depths exceeding 3 km, this block is subducting beneath the Calabrian Arc. Much of its structure is obscured by a dense accretionary prism (Gutscher *et al.*, 2017; Tugend *et al.*, 2019).

GPS measurements in the Central Mediterranean show a NW-directed regional stress field, driven by the 5 mm/yr^{-} convergence of the African plate (Hollenstein et al., 2003; Serpelloni *et al.*, 2007). The stress has deformed the northern tip of the HMP indenter in SE Sicily (Cogan *et al.*, 1989; Pedley and Grasso, 1992) and generated strain about 150 km away from the collision front, along the NW–SE trending, <30 km wide Malta Horst (Fig. 1b). Early-stage deformation is characterized by the development of synthetic and antithetic shears, alongside secondary synthetic strike-slip and normal faults (Tchalenko, 1970), producing a hierarchy of first-, second-, and third-order strike-slip faults (Moody and Hill, 1956). The thin-skinned shearing is associated with the underlying principal displacement zone (PDZ), which is characteristically oriented oblique to the maximum principal stress (σ_1) (Sylvester, 1988). Sustained convergence results in thrust systems, often in en echelon arrangements, and shortening of existing intraplatform grabens by basin inversion (Bally, 1984; Bonini *et al.*, 2012; Zwaan *et al.*, 2022). Deep-seated basement faults may seed this thin-skinned thrusting and localized folding (Butler *et al.*, 2025). Within these settings, low-friction lithologies, such as evaporites, serve as critical décollement surfaces, facilitating the translation and folding of the sedimentary cover (Letouzey *et al.*, 1995).

This study describes the neotectonics of the Malta Horst area that entered a foreland position since the Miocene (Dart *et al.*, 1993; Maiorana *et al.*, 2023). The Malta Horst is bounded by a set of conjugate normal faults, here named the Sikka Fault and the Hurd Bank Fault, along its NE margin and by the Maghlaq fault system (Bonson *et al.*, 2007; Illies, 1981) along its SW margin. The horst is adjacent to the >500 m deep Pantelleria Rift (Fig. 1b) bounded by the Malta Graben Fault that trends NW but makes a sharp change in direction to W–E south of Gozo (East Malta Graben Fault). The Maltese Islands are the only subaerial part of the Malta Horst (Fig. 1c) located along the northern margin of the 200 km-wide, Malta-isolated carbonate platform (MICP), which aggraded >6 km of Jurassic to Oligocene carbonates over Permo-Triassic continental siliciclastics and carbonates (Fig. 1d) until it drowned by the end of the Oligocene (Gatt, 2022). The MICP was along a passive margin bounded by the Malta and Medina escarpments and was tectonically segmented by NE–SW-trending faults that formed a series of ridges and basins described in (Gatt, 2025). The <1.1 km-thick Cenozoic succession comprises seven formations, which are here subdivided into thirteen facies associations named TA to TL (Table 1). The top six Oligo-Miocene formations are exposed in the Maltese Islands.

A synthesis of previous research on the Cenozoic tectonics of the Malta Horst, *e.g.*, Gatt (2022); Grasso *et al.*, (1986); Grasso and Pedley (1985); Illies (1981); Martinelli *et al.*, (2019); and Pedley *et al.*, (1976, 1978), allows for the classification of regional deformation into four distinct tectonic phases (A to D) spanning the Late Oligocene to the

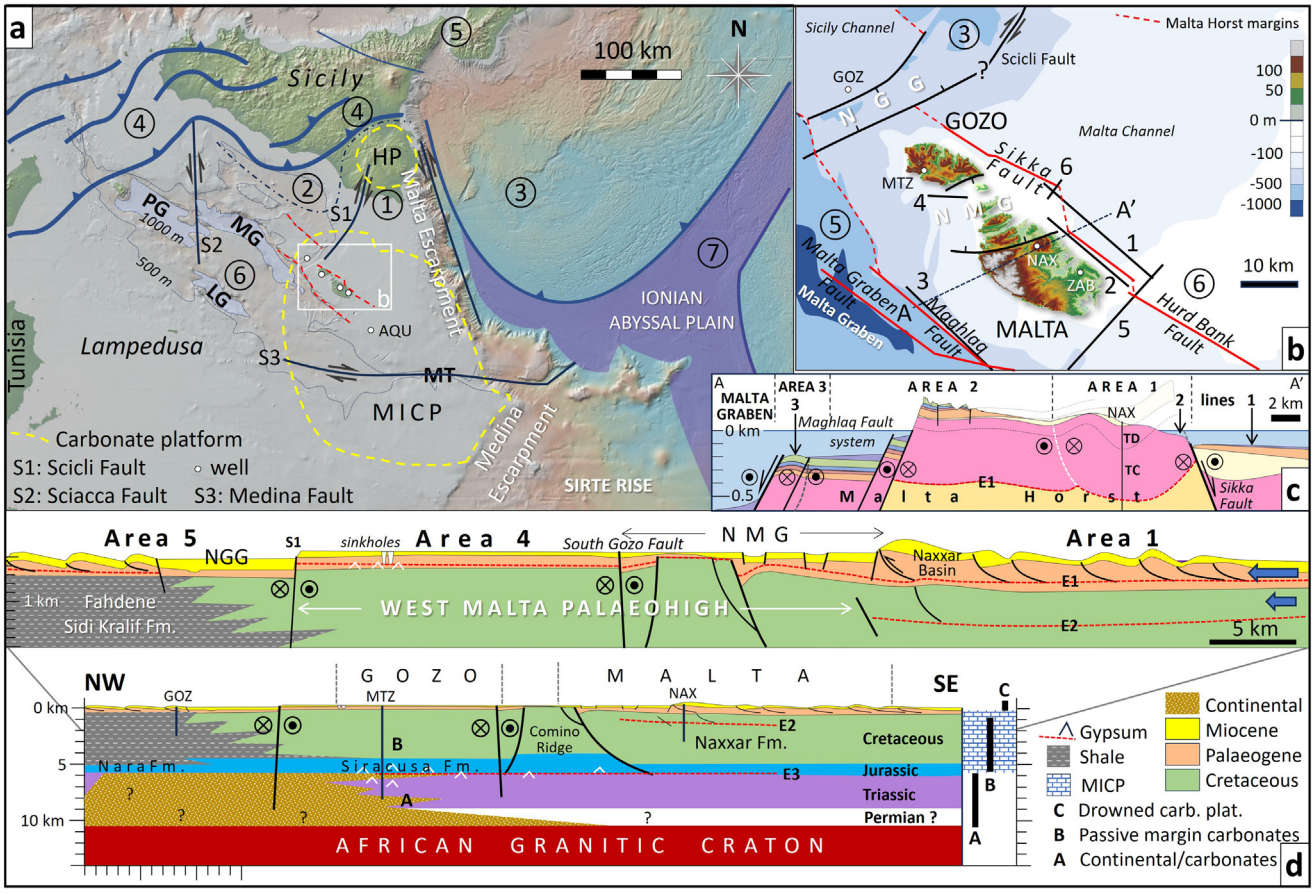

Fig. 1. Dashed yellow line shows the extent of carbonate platforms: MICP and HP (Hyblean carbonate platform) in the Central Mediterranean. (a) Main geotectonic features marked by the circled numbers: 1. Hyblean-Malta Plateau (HMP) bounded on the south by the Medina Wrench (S3) and on the west by the Scicli Fault (S1), 2. Gela Basin (foredeep) bound on the west by the Sciacca Fault (S2), 3. Ionian crust overlain by an accretionary prism, 4. Sicilian-Maghrebian thrust belt, 5. Calabrian Arc, 6. Pantelleria Rift and main grabens: Pantelleria Graben (PG) is separated by the Sciacca Fault (S2) from the Linosa Graben (LG), Malta Graben (MG), and the Medina Trough (MT), 7. Ionian oceanic crust. (b) Maltese Islands: North Gozo Graben (NGG), North Malta Graben (NMG), location of seismic lines 1 to 6, and main faults (in red) and wells mentioned in the text. (c) Cross section A-A' along the Cenozoic foreland succession of the Malta Horst (legend for lithology in Fig. 2). (d) Generalized NW–SE cross-section along Malta Horst showing influence of WMP basement on thrusting (no erosion shown). Stratigraphy based on MTZ and NAX wells.

Pliocene. These tectonic phases have impacted the development of the present phase E contractional deformations deduced from offshore seismic lines, cross sections, and well data in the foreland area. The focus of this study is phase E neotectonic contraction in the Malta Horst. Previous studies on neotectonics are limited to small areas of the Malta Horst (*e.g.*, Gardiner *et al.*, 1995; Reuther, 1984), whereas this study encompasses a wider area that includes reactivated older faults and new structures observed in seismic imaging along the margins of the Malta Horst, which correlate to the hitherto enigmatic dome-shaped topography along the NE coast of Malta Island, described for the first time in the context of anticlinal and synclinal structures. The regional stress field agrees with the plate motion vectors showing ongoing NW compressive deformation in the central Mediterranean and may result in potential geohazards in Malta.

The foreland deformations since the Miocene are conceptualized within the context of the temporal change in the rate of migration by the Calabrian Arc with respect to the converging African plate, which is key to understanding when contraction or extension prevailed in the central Mediterranean. The objective of this study is to: (1) review the chronology of extensional and contractional phases in the MICP foreland, (2) describe the reactivation of old normal faults by transcurrent movement and the anticlinal and synclinal structures in Malta, (3) assess the role of evaporites in folding and basin inversion tectonics, and (4) discuss the relationship of the Hyblean-Malta Plateau foreland within the geodynamics of the Central Mediterranean.

2 Geological setting

The MICP developed since the Mesozoic on the North African passive margin (Jongsma *et al.*, 1985) (Fig. 1a) along an abortive rift bounded by the Medina Escarpment (Gatt, 2025) in conjunction with the rifting of the Ionian oceanic crust (Speranza *et al.*, 2012; Tugend *et al.*, 2019). The deep wells confirm >6 km of mostly carbonates in the MICP succession, interbedded by four extensive evaporite beds and two <200 m thick shale beds (lower Jurassic and top Triassic) of continental

Table 1. MICP sediments: Stratigraphy, facies associations (FA) and main seismic reflectors.

Period/*Epoch*	Group		Formation	*Member*	Thickness	FA	Lithology	Depositional environment (depth in m)	
Plio-Quat.			San Leonardo		10 m	TL	Mudstone, rudstone and clay	Shallow marine/ karst	M
Miocene	Malta Group		Messian evaporites		0 to >100		E0 gypsum: found along margins of MICP and in basins	subaerial	
			Upper Coralline Limestone		<60	TK	Limestone: Coralline red algae, coral	Shallow marine carbonates (<50 m)	BC
			Greensands		0-13	TJ	Glauconitic limestone with LBF		
			Blue Clay		15-75	TI	Marl	Deep marine (>200 m)	
			Globigerina Limestone	*Upper*	8-26	TH	Limestone: wackestone/packstone	Pelagic carbonates (>150 m)	
				Middle	15-38	TG	Chalk capped by C_2 phosphorite bed		
				Lower	2 to <200	TF	Limestone: wackestone/packstone		O
Oligocene			Lower Coralline Limestone	*Xlendi & Mara*	2-30	TE	Limestone: LBF, echinoids, bryozoans	Carb. Plat. slope (>40 m)	
				Migra Ferha	40-60	TD 2	Limestone: Coralline red algae (CRA), rhodoliths, echinoids	Open marine carbonate platform (<40 m)	C
				Attard	<25	TD 1	CRA, large benthic foraminifera (LBF), coral		
				Maghlaq	100-400	TC	Limestone/dolomite: micrite and miliolids, and argillaceous limestone/marl in basins	Carbonate platform interior (<20 m) and sabkha	E
Eocene			Zabbar		90-360	TB TA	Dolomite/limestone, *Alveolinid* packstone capped by E1 gypsum bed		
Paleocene			unnamed		0 -500?		absent in Malta area and over MICP palaeohighs		K
Cretaceous	Naxxar		Upper Naxxar		<1000		Dolomite, gypsum (capped by lignite)	Carbonate platform interior (<30 to 0 m)/sabkha/ karst	
			Lower Naxxar		>2500		Dolomite, gypsum		

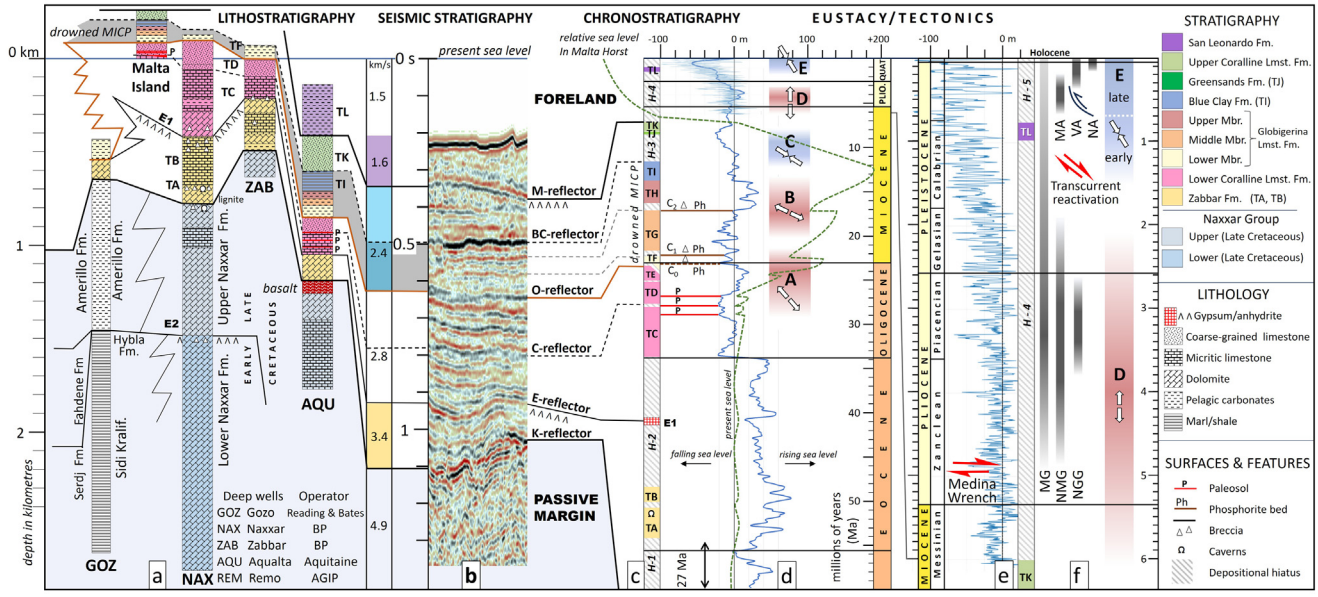

Fig. 2. Stratigraphy of the MICP. (a) Stratigraphy of the MICP. (b) Seismic velocity and main reflectors around the AQU well. (c) Cenozoic stratigraphy of MICP. (d) Global sea level curve based on Miller *et al.* (2020) and tectonic phases A to E. Dotted green line shows relative sea level in Malta Horst. (e) Plio-Quaternary eustacy (Miller *et al.*, 2005) and stratigraphy. (f) Timing of growth of Malta Graben (MG), North Malta Graben (NMG), North Gozo Graben (NGG) and Marsascala Anticline (MA), Valletta Anticline (VA), and Naxxar Anticline (NA).

provenance at the base (Gatt, 2025) related to formations encountered in North Africa (Fig. 1d). The youngest two evaporite beds were deposited along the Eocene-Oligocene boundary (E1 evaporite bed) and during the Messinian (E0 evaporite bed). The depositional style, absence of siliciclastic deposits, and positive bathymetry over surrounding pelagic sediments identify the Maltese carbonates as an isolated carbonate platform (Gatt, 2012; Rusciadelli and Shiner, 2018; Gatt, 2022) comparable to ancient buildups identified in seismic (Burgess *et al.*, 2013). Jurassic to Cretaceous passive margin extension produced steep faulted margins along the MICP with a throw of 0.5 to >1 km along the NNW-trending Malta Escarpment on the east and along the Medina Escarpment in the SE (Finetti, 1982; Jongsma *et al.*, 1985; Tugend *et al.*, 2019; Gatt, 2025). Well data (Fig. 2a) confirm that the >2 km thick Naxxar Formation (Cretaceous) consists of shallow marine carbonates with gypsum/anhydrite beds (E2 evaporite bed) (Dart *et al.*, 1993; Gatt, 2022).

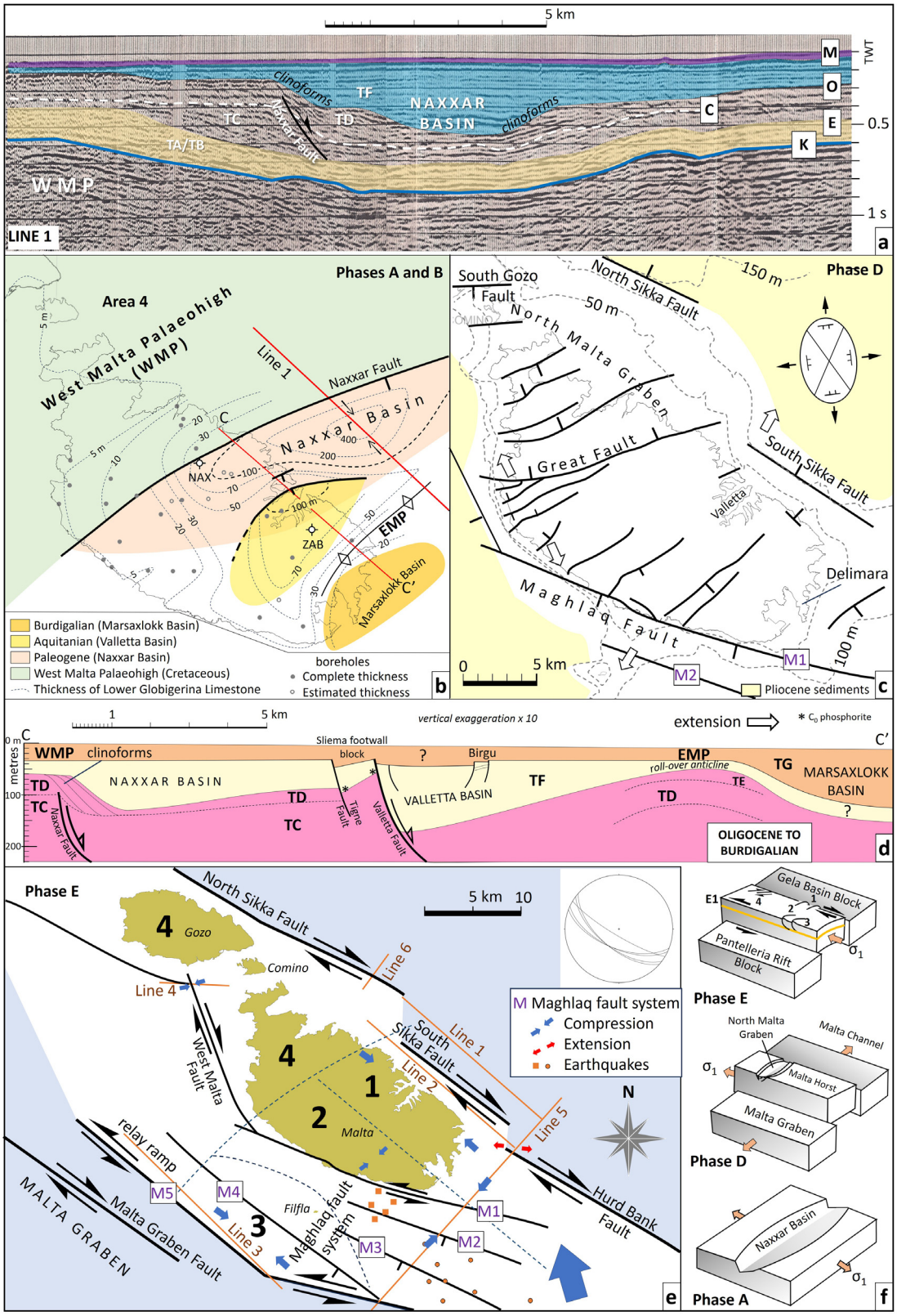

Fig. 3. Tectonic phases A to D: (a) Seismic line 1 showing the undeformed Naxxar Basin (phase A); (b) Palaeomap showing the West Malta Palaeohigh (WMP) and the growth of the Naxxar and Valletta basins (phase A) and Marsaxlokk Basin (phase B); (c) Phase D NW and NE trending faulting by N–S extension; (d) Palinspastic reconstruction of cross section C-C' showing development of basins in phases A and B. (e) Phase E faulting and Areas 1 to 4. Square dots are earthquakes occurring in 2015 (Bozionelos *et al.*, 2017), (f) Models of deformation during phases A, D, and E.

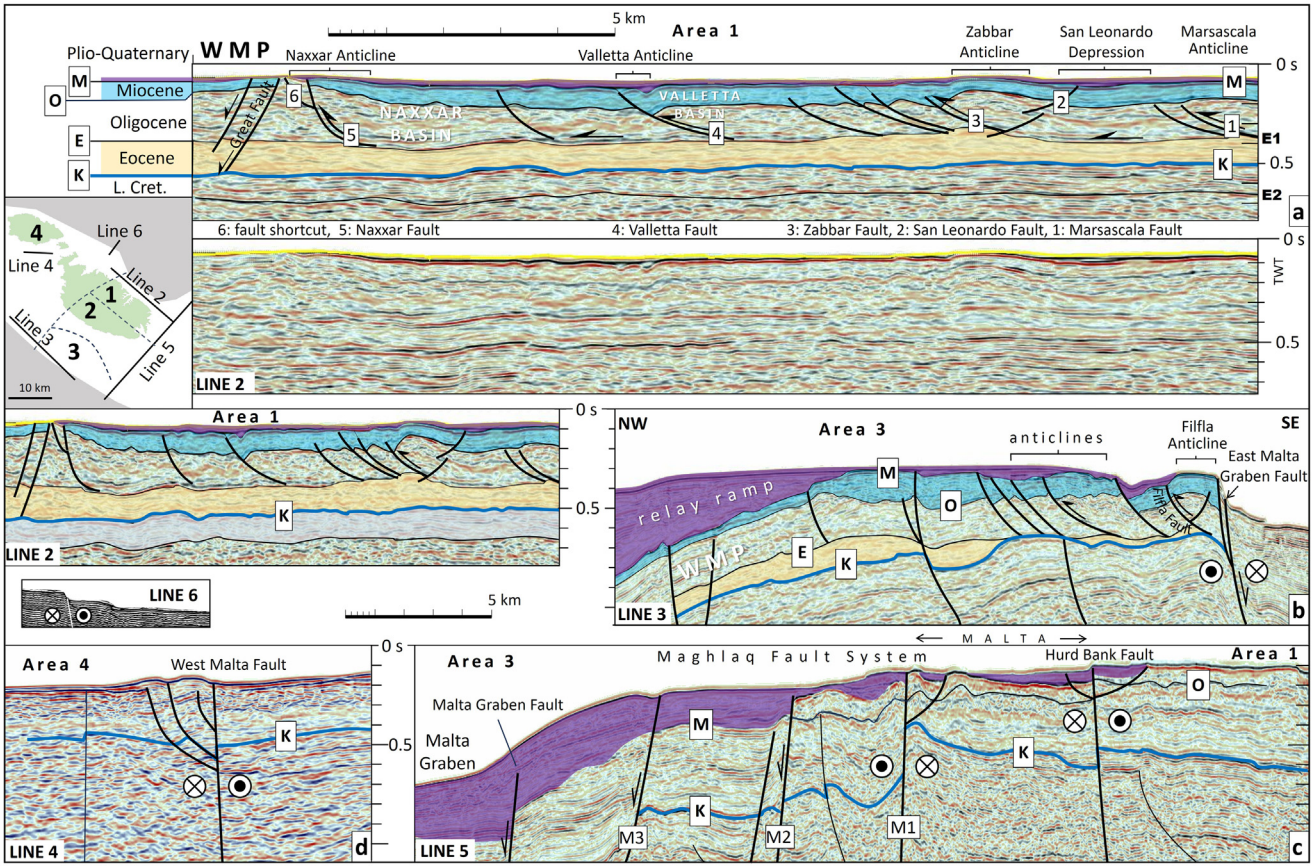

Fig. 4. Map of Areas 1, 2, 3, and 4 and location of seismic lines 2 to 6. (a) Interpreted and uninterpreted seismic line in Area 1. (b) Seismic line 2 showing thrusts that sole along E1 gypsum bed. Seismic line 3 showing relay ramp produced during Phase D. (c) Seismic line 5 showing negative flower structure over Hurd bank Fault and positive flower structure over Maghlaq Fault. (d) Positive flower structure over West Malta Fault (b, c, and d same scale).

The switch from the Mesozoic passive margin to continental convergence of Africa with respect to Eurasia in the Late Cretaceous (Dewey *et al.*, 1989; Ricou, 1994; Rosenbaum *et al.*, 2002) produced a regional compressive event over northern Africa (Guiraud and Bosworth, 1999; Roure *et al.*, 2012) that is equivalent to the Santonian to Paleocene H-1 depositional hiatus over the MICP (Gatt, 2022) (Fig. 2c). The compression produced the inversion of the Mesozoic basin along the footwall block (Comino Ridge) described in Gatt (2025). The Comino Ridge and the adjacent inverted basin form the culmination of the West Malta Palaeohigh (WMP) that underlies an area extending from Gozo to the North Malta Graben (Fig. 1d). Pelagic carbonates of the Lower Globigerina Member (Miocene) thin to <30 m over the WMP (Fig. 3b), whereas the Middle Globigerina (TG) is entirely missing over eastern Gozo (Pedley *et al.*, 1976).

During the early Cenozoic, narrow mobile arcs began to migrate and consume, by subduction, large parts of the Neotethyan oceanic crust (Faccenna *et al.*, 2004; Malinverno and Ryan, 1986; van Hinsbergen *et al.*, 2020). The Calabrian Arc reached the Central Mediterranean by the Neogene (Ciarcia and Vitale, 2024; Jolivet and Faccenna, 2000), producing the accretion of the Sicilian-Maghrebian Thrust Belt (Speranza *et al.*, 2018) that began to override the Pelagian sector of the North African plate (van Dijk and Scheepers, 1995). The Malta Group (Cenozoic) sediments (Table 1) reflect the interplay between tectonics and global eustasy based on the sea level curve of Miller *et al.* (2020) (Fig. 2d). The late Eocene is marked by the E1 gypsum bed that thickens toward the NW, where its dissolution resulted in 300 m-wide sinkholes along the coast of western Gozo (Gatt, 2019) and large caverns encountered at about 600 m depth in the onshore Naxxar deep well. Based on published studies, e.g., Gatt (2022); Grasso *et al.*, (1986); Grasso and Pedley (1985); Illies (1981); Martinelli *et al.*, (2019); Pedley *et al.*, (1976, 1978), the Cenozoic tectonics of the Malta Horst are here categorized into five tectonic phases (A to E in Fig. 2d), with the present neotectonic phase E being the subject of this study:

2.1 Phase A (Chattian to Aquitanian)

The NW–SE extension during the deposition of the Chattian drowning succession (facies associations TD and TE) of the Lower Coralline Limestone Formation produced the Naxxar Fault, which is a 13 km-long normal fault along the

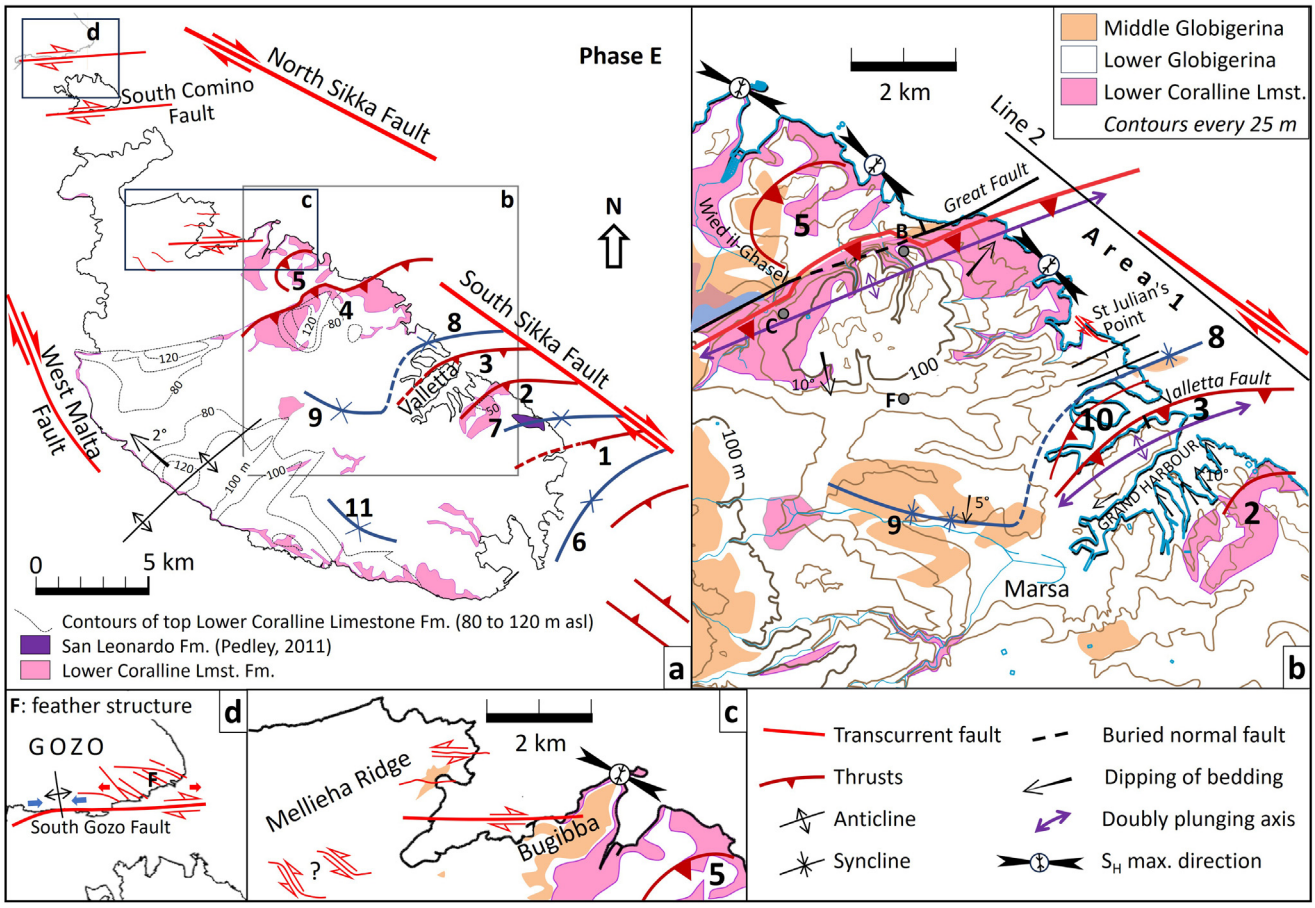

Fig. 5. (a) Phase E compressive deformation in Area 1: 1. Marsascala Anticline, 2. Zabbar Anticline, 3. Valletta Anticline. 4. Naxxar Anticline, 5. Ghallis Anticline, 6. Marsaxlokk Syncline, 7. San Leonardo Syncline infilled with Calabrian carbonates, 8–9. Sliema-Hamrun Syncline, 10. Pieta Anticline, and 11. Mqabba Basin (Area 2); (b) Inset of Area 1 showing topography and dip of beds and location of Wied il-Ghasel paleoriver mentioned in the text. The orientation of S_H max is from Grasso *et al.* (1986); (c) inset showing left-lateral strike-slip faults along Mellieha Ridge and Bugibba (Area 4). (d) South Gozo Fault is a dextral strike-slip fault showing anticline (compression) on the west and feather structures (extension) along the east.

WMP footwall block (Fig. 3a, 4a) that bounds the Naxxar Basin (Gatt, 2022, 2025) imaged in seismic line 1 as a <7 km-wide depression (Fig. 3a) partly filled with prograding clinoform bedding of facies association TD. Neptunian dykes developed around the margins of the depocenter that were later filled with phosphorite conglomerate (Gatt, 2005) when the MICP drowned by the late Chattian (Gatt *et al.*, 2009). The underfilled Naxxar Basin was later filled with pelagic carbonates of the Lower Globigerina Member (TF) that thicken along the hanging wall from >60 m over Malta Island (locality F in Fig. 5b) to 400 m in the offshore depocenter imaged in seismic as post-kinematic horizontal reflectors that unconformably onlap the Oligocene sediments. Although the Naxxar Fault is blind in Malta, locality D close to the fault tip shows the erosive surface along the margin of the footwall block and the overlying transgressive wedge (Fig. 6h).

Nested in the SE margin of the Naxxar Basin is the 5 km wide Valletta Basin, which was first described by Pedley *et al.* (1976) as an area with a thick succession of Lower Globigerina Limestone, which is an important source of building stone in Malta (Gatt, 2006). The Valletta Basin developed as a half graben during the Aquitanian after the MICP drowned at the end of phase A. It is bounded by the Valletta Fault in the west along the Sliema footwall block (locality G). Borehole data confirms that the Valletta Basin is filled with >100 m of pelagic sediments (locality H in Fig. 4a) of the Lower Member of the Globigerina Limestone Formation (TF) that thin to <30 m along the upper slope of the rollover anticline forming the East Malta Palaeohigh (EMP). Figure 3d is a palinspastic reconstruction of the Naxxar and Valletta basins filled with Aquitanian to Burdigalian pelagic sediments. Synthetic faults to the Valletta Fault are exposed along the Valletta peninsula close to locality H (Fig. 6i) whereas the slope of the hanging block in Birgu is filled with pelagic sediments dipping 10° toward the basin depocenter.

2.2 Phase B (Burdigalian)

Late early Miocene WNW–ESE extension during the Aquitanian lasted till the Burdigalian and is associated with

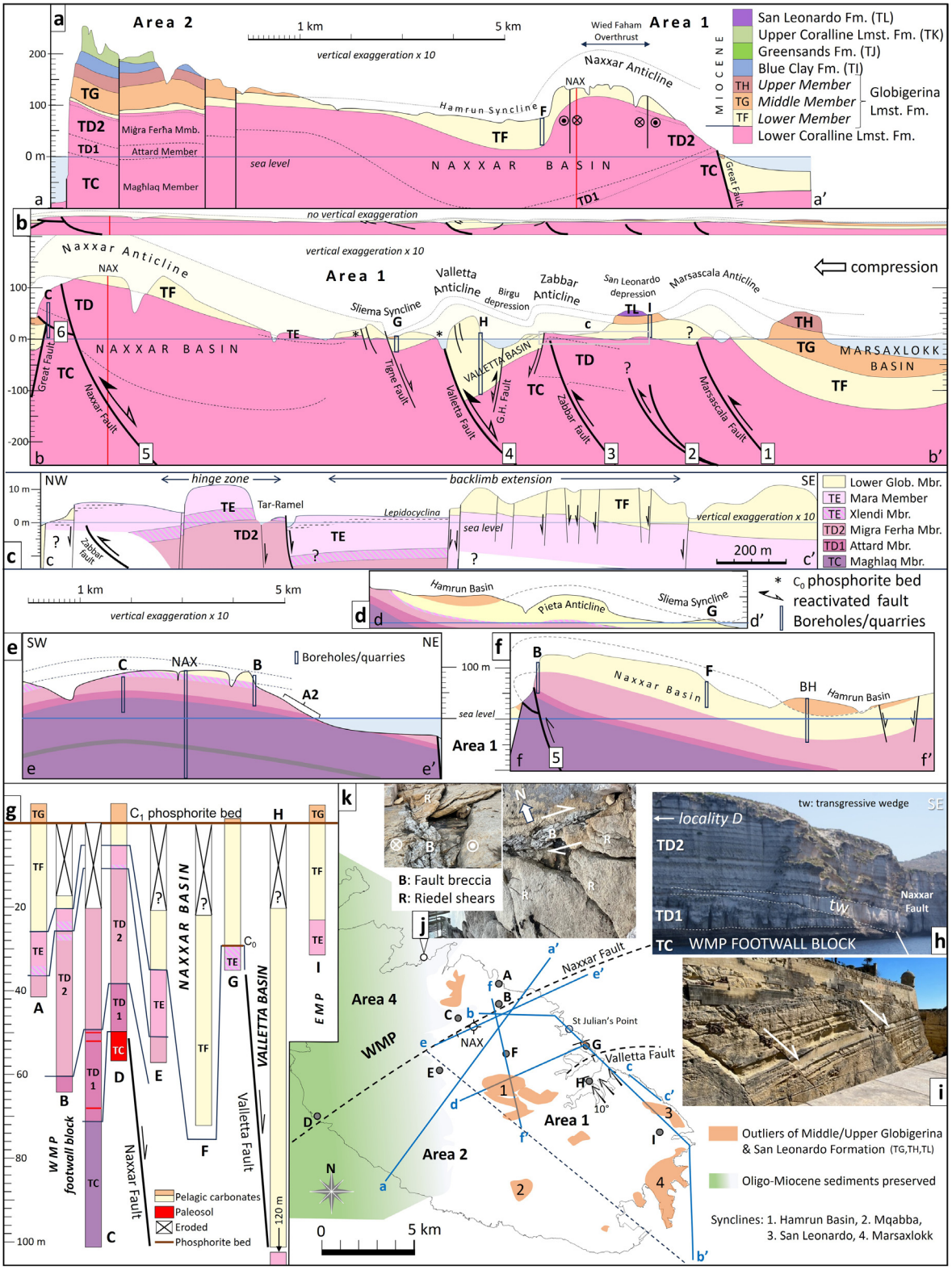

Fig. 6. Cross sections, outcrops, and borehole data (locations shown in map). (a) Cross section a-a' showing five Oligo-Miocene formations in Malta; (b) Cross section b-b' showing inversion tectonics along NE coast of Malta (top cross section has no vertical exaggeration). Thrusts 1 to 6 are shown; (c) cross section c-c' of crest of Zabbar anticline with TD2 exposed; (d) cross section d-d' through Hamrun-Sliema syncline; (e and f) cross-sections e-e' and f-f' through Naxxar Anticline; (g) stratigraphic logs of boreholes and outcrops A to I; (h) photograph of erosion along margin of Naxxar Fault footwall close to locality D; and (i) series of faults synthetic to Valletta Fault close to locality H. (j) Map of cross sections and outliers.

the growth of small normal faults and basins (Martinelli *et al.*, 2019) filled with pelagic sediments of the Middle Member of the Globigerina Limestone (TG) capped by phosphatic conglomerate filling Neptunian dikes (Dart *et al.*, 1993). The most prominent feature is the Marsaxlokk Basin seen in seismic imaging (Fig. 4a), which began to develop in the late Aquitanian and peaked in the Burdigalian in SE Malta. The basin shows a thickening of the middle Globigerina sediments to <100 m, dipping SE, presently preserved as an outlier around the Delimara peninsula (Fig. 6k) (Baldassini and Di Stefano, 2017).

2.3 Phase C (Tortonian)

The Tortonian compressive event coincides with the H-3 depositional hiatus that terminates the deposition of pelagic marls of the Blue Clay Formation (TI), marking the end of the Serravallian (Hilgen *et al.*, 2009). The regional NW compression produced inversion of older basins in the Ionian Abyssal Plain during the Tortonian (Gallais *et al.*, 2011) and significant uplift of the MICP. Bialik *et al.* (2021) speculate a major uplift of >500 m that permitted the return of shallow marine carbonate sedimentation (TJ and TK) in the Maltese Islands. However, the geodynamics of this phase remain uncertain in the MICP.

2.4 Phase D (Messinian to Pliocene)

The approaching Calabrian arc produced foreland extension in the Sicily Channel due to the slab-pull effect (Argnani, 1990). Most authors also consider the Pantelleria Rift to have begun to develop in the late Miocene to early Pliocene (Argnani, 1990; Civile *et al.*, 2021; Dart *et al.*, 1993). In the Maltese Islands, the N–S extension produced two sets of NE and NW trending faults (Fig. 3c) that control most of the present topography and surrounding bathymetry (Vossmerbäumer, 1972; Illies, 1981; Dart *et al.*, 1993; Bonson *et al.*, 2007):

1 A set of NE-SW trending faults with a throw of <200 m associated with high extensional strain (Putz-Perrier and Sanderson, 2010) that produced the North Gozo Graben in offshore NW Gozo and the North Malta Graben (Fig. 1b). The latter comprises a series of parallel horsts and grabens, bounded by the South Gozo Fault and the Great Fault that bisects the entire island of Malta (Fig. 3c).
2 The second set of faults consists of NW–SE trending, conjugate normal faults that form the margins of the Malta Horst: (i) the Sikka Fault along the NE margin with a vertical offset of <100 m (Fig. 3c) and (ii) along the SW margin is the Maghlaq fault system (Bonson *et al.*, 2007; Dart *et al.*, 1993), where SW–NE extension produced downthrown blocks that are presently mostly submerged (Fig. 1c), here sub-divided by five main faults: the inner M1 fault (displacement >200 m) that reaches southern Malta, to the outer M5 fault that is parallel to the Malta Graben Fault (Fig. 3e), with an overall vertical offset of >1 km. The M4 and M5 faults interact along a NW-dipping relay ramp observed in seismic line 3 (Fig. 4b), which was later filled by a thick wedge of post-kinematic Plio-Quaternary sediments.

Footwall upwarping of the Malta Horst along the Maghlaq Fault resulted in the Plio-Quaternary emergence of the Maltese Islands (Illies, 1981), where Pliocene sediments are absent (Gatt, 2007). At the end of phase D, the Messinian drawdown of sea level resulted in a thick evaporite succession in Mediterranean basins (Hsu *et al.*, 1973) and exposed the Malta area to subaerial conditions during the H-4 depositional hiatus, which persists in the Maltese Islands as the H-5 depositional hiatus (Fig. 2f).

3 Data and methods

The stratigraphy is reconstructed using nine measured sections in localities A to I (Fig. 6g), 18 localities logged by Gatt (2022), boreholes in the Maltese Islands from the Minerals Assessment Report (1996), and water borehole data from Pedley *et al.* (1976). Limestone texture is based on Dunham (1962) and Embry and Klovan (1971)classifications. Data from deep wells is from the onshore Naxxar-2 (NAX), Zabbar (ZAB), and Madonna Taz-Zejt (MTZ) wells and the offshore Gozo (GOZ) and Aqualta (AQU) wells (locations in Fig. 1 a, b) that have penetrated Cenozoic to Cretaceous sediments. The Paleogene biostratigraphy of the NAX and ZAB wells is reinterpreted by Gatt (2012) in the context of a more recent biozonation scheme based on benthic foraminiferans by Cahuzac and Poignant (1997) and Serra-Kiel *et al.* (1998), which is used to date the sediments.

Six seismic reflection lines are used to interpret the structures affecting the MICP. Seismic line 1 lies just outside the Malta Horst and is from a survey carried out in 1980 for the Government of Malta, whereas seismic lines 2, 3, 4, and 5 (Fig. 1b) are part of a 2D seismic grid produced by TGS-NOPEC Geophysical Company in 2000–2001, which consists of the Malta Sicily Channel (MSC01) and the Malta Medina Bank (MB01) datasets. The main seismic reflectors and the seismic velocity to depth conversion are based on data from the AQU well (Fig. 2b), which is correlated to rock outcrops and deep wells in Malta. The methodology used in this study is based on the correlation of the geometry of structures seen in seismic line 2 with the topography of the NE coast of Malta. Present *in situ* strain measurements of near-surface stress in Malta are from Grasso *et al.* (1986) using the doorstopper method.

4 Results

4.1 Main seismic discontinuities

The data collected from wells and outcrop localities A through I are used to interpret offshore seismic lines and construct geological cross sections on land. Six strong reflectors, M, B-C, O, C, E, and K-reflectors described by Gatt (2025), are identified in seismic lines (Fig. 2b and Table 1), which correlate to lithological boundaries that mark depositional hiatuses H-1 to H-4, of which H-3, H-4, and H-5 are observed in the Maltese Islands (Fig. 2c). The six reflectors within the Malta Group (Cenozoic) are bounded by the M-reflector at the top and the K-reflector at the base, with the intermittent E-reflector having an important role:

M-reflector: marks the Messinian drawdown of sea level that produced subaerial conditions over large parts of the Mediterranean (Hsu *et al.*, 1973; Krijgsman *et al.*, 1999; Roveri *et al.*, 2014), corresponding to the H-4 depositional hiatus in the MICP that terminates sedimentation in the Upper Coralline Limestone Formation (TJ and TK), which consists of shallow marine carbonates (Pedley, 1978). The M-reflector is capped by Plio-Quaternary sediments along the margins and outside the Malta Horst.

O-reflector: corresponds to the termination of shallow marine sedimentation when the MICP drowned and was draped by pelagic sediments of the Globigerina Limestone Formation (facies association TF).

C-reflector: marks the abrupt change from interior, fine-grained carbonate platform sediments (facies association TC) to coarse-grained drowning succession (TD).

E-reflector: corresponds to the E1 gypsum bed, an evaporite bed deposited in a sabkha type of environment capping the Ypresian shallow marine carbonates of the Zabbar Formation consisting of *Alveolina* packstones (Gatt, 2022). The age of the gypsum bed may range from middle to late Eocene and was deposited during the circa 15 Ma long H-2 depositional hiatus.

K-reflector: The H-1 depositional hiatus marks a 27 Ma-long biostratigraphy gap that terminates Cretaceous carbonate sedimentation of the Naxxar Group (Gatt, 2022). The horizon is characterized by cavernous porosity, breccia, and a thin lignite bed encountered in NAX and ZAB wells, which suggests a karstic surface along the exposed MICP, which was uplifted by compression that resulted in anticlinal structures (Gatt, 2025). Several thrusts are observed in seismic along the topmost Naxxar Formation (Cretaceous) resulting from compression during phase C.

Several structures occur in different parts of the Malta Horst, which is here subdivided into five areas (Fig. 4) based on the type of structures. This study focuses on deformation along the NE margin (Area 1) of the Malta Horst that extends from the Sikka Fault to a series of domes and ridges along a $<$10 km wide belt along the NE coast of Malta Island.

4.2 Area 1

Tectonic Phase E resulted in differential deformation across the various segments of the Malta Horst.

Faults:

The NE margin of Area 1 is bounded by the Sikka Fault and the Hurd Bank Fault, south of Malta. The latter is a right-lateral strike-slip fault seismically imaged by line 5 (Fig. 4c), showing a negative flower structure. The NW-trending south Sikka Fault developed as a normal fault during phase D (Line 6) but is now reactivated as a right-lateral strike-slip fault (Fig. 3e).

Contractional deformation:

Seismic line 2 shows a series of thrust faults dipping $<$40° with overlying anticlines (Fig. 4a). The position of these anticlines in seismic imagery correlates with $<$4 km wide topographic highs observed along the NE coast of Malta where the Lower Coralline Limestone Formation is $>$50 m above sea level (Fig. 5a). Felix (1973) and Pedley *et al.* (1976)describe these hitherto enigmatic folds in Malta as the "Naxxar Dome" and Zabbar culmination, where the Lower Coralline Limestone Formation in these areas reaches 120 and 50 m asl, respectively. However, no explanation is given for their formation, although they are known to be associated with positive gravity anomalies (Harrison, 1954), implying that older and denser rock is closer to the surface. These gravity anomalies attracted the drilling of the first onshore hydrocarbon dry wells, namely, the NAX and ZAB dry wells in the 1950s.

Cross-sections in Figure 6 are based on well data and measured outcrops in Malta within Area 1 and show a series of anticlinal and synclinal structures along the NE coast of Malta overlying six thrust faults labeled 1 to 6 in Figure 6b, where the Naxxar Dome and the Zabbar culmination are interpreted as the Naxxar and Zabbar anticlines. The emergent thrust system is extensively eroded in SE Malta, where the topography created by anticlines is mostly obliterated but more preserved toward the NW. The thrusting resulted in basin inversion and uplift so that the top of the Lower Coralline Limestone Formation is presently 120 m asl (thrust 4 in Fig. 5a). A succession of four main anticlines separated by synclines that extend from the SE to the NW in Area 1 is observed:

4.2.1 Marsascala Anticline and Marsaxlokk Basin

A nearly symmetrical anticline (thrust 1) is observed in seismic imagery (Fig. 3b) with its western end emergent on land. Contraction along the Marsascala thrust fault uplifted Oligo-Miocene sediments, exposing the Lower Coralline Limestone Formation along Marsascala Bay. In seismic line 2, the thrust fault soles along the E1 evaporite bed (Fig. 4a), and Miocene pelagic sediments show some thinning over the anticline, which suggests Messinian erosion. The slight bathymetric shallowing over the anticline implies post-Messinian uplift. The NW margin of the Marsaxlokk Basin is partly subaerial along the Delimara Peninsula, where it forms the dorsal part of the Marsascala Anticline. The exposed Middle and Upper members of the Globigerina Limestone dip toward the SE in the direction of a depression that formed by Burdigalian extension (Fig. 6b).

4.2.2 Zabbar Anticline and San Leonardo Syncline

In seismic imaging (Fig. 4a), the Zabbar Anticline forms the frontal part of the imbricate thrust system involving Oligo-Miocene sediments that extends to the Marsascala Anticline. Thrust faults 2 and 3 (Fig. 6b) sole along the E-reflector gypsum bed decollement with the overlying synkinematic Miocene pelagic sediments mostly preserved. On land, erosion has exhumed facies association TE along the emergent Zabbar Anticline and the underlying Migra Ferha Member (TD2) at Tar-Ramel along the anticline hinge zone (Fig. 6c). The back limb of the anticline is fractured by extension, which produced several $<$50 m wide grabens passing laterally to the syncline farther east, here named the San Leonardo Depression. This paleobathymetric low between the Zabbar and Marsascala anticlines accumulated the shallow marine carbonates of the San Leonardo Formation, deposited at depths of 10 to 30 m (TL) during the Calabrian sea level highstand (Pedley, 2011). The relatively resistant San Leonardo carbonates unconformably cap and preserve the much weaker underlying Middle Globigerina limestone.

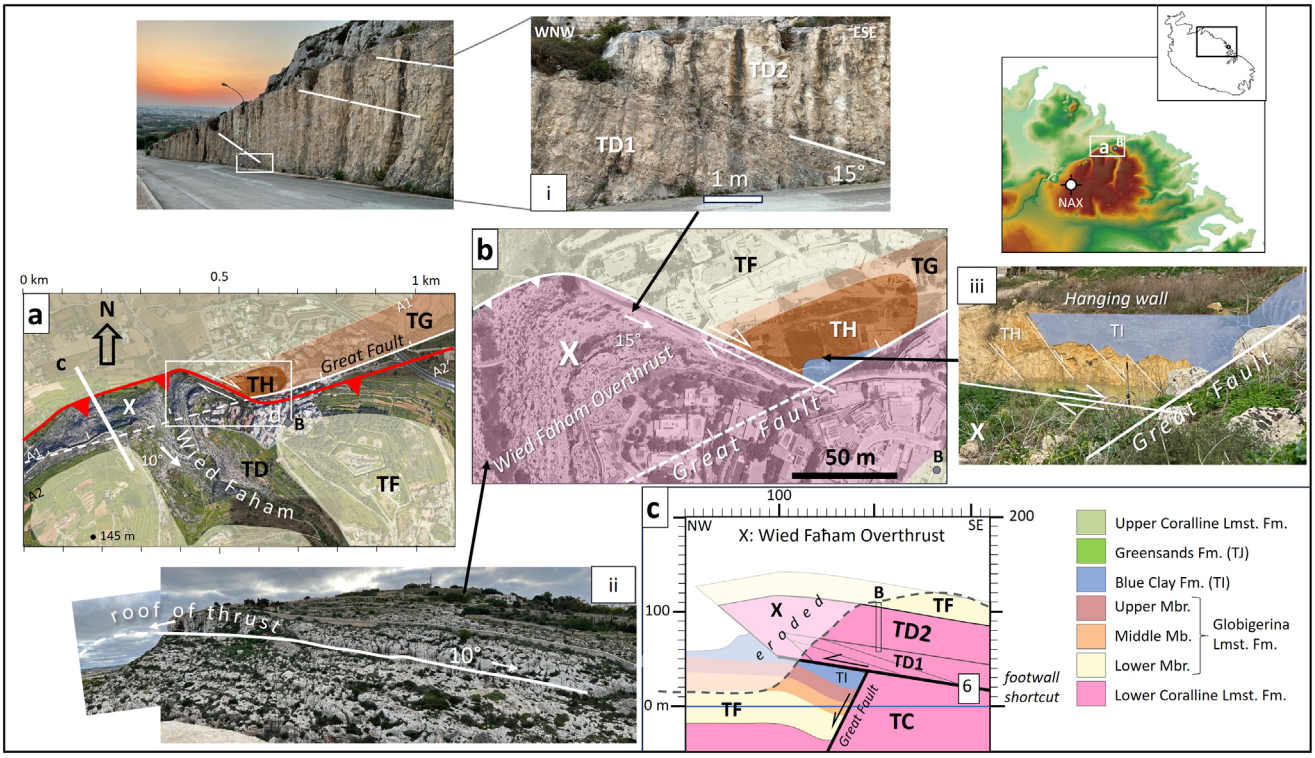

Fig. 7. The Wied Faham Overthrust (denoted by X) within the Naxxar Anticline: (a) Map showing location of overthrust in relation of Great Fault, (b) Lithology of Wied Faham Overthrust with accompanying photographs: (i) the 15° dip of floor thrust exposed along road cut, (ii) the 10° dip of roof thrust along Wied Faham and (iii) antithetic faults to the Great Fault draped with Blue Clay adjacent to the overthrust X. (c) Cross section of overthrust X interpreted as an overturned fold that downflexed the hangingwall of the Great Fault. The loading of the hanging wall of Great Fault preserved an outlier of Upper Globigerina Limestone (TH) with clay (TI).

4.2.3 Valletta Anticline

The Valletta Fault (thrust 4) and its 1 km apart, antithetic Grand Harbour Fault were reactivated as reverse faults during phase E (Fig. 6b). Both faults are presently submerged but can be inferred by the geometry of the sediments. Contraction resulted in basin inversion that raised the Valletta Basin depocenter to 50 asl, which is 20 m higher than the adjacent, pre-inversion footwall block in Sliema (Fig. 6b). The nearly symmetrical, doubly plunging, NE–SW trending Valletta Anticline presently forms the backbone of the Valletta Peninsula, composed of the Lower Globigerina Limestone (TF). East of the Grand Harbour Fault, the Birgu Depression preserves the basinward-dipping pelagic (TF) sediments exposed at Birgu along the undeformed upper hanging wall slope of the Valletta basin.

4.2.4 Naxxar Anticline and Sliema-Hamrun Syncline

The cross sections of the Naxxar Anticline (Fig. 6a, b, and f) show a noncylindrical anticline that doubly plunges inland to the SW and to the NE (Fig. 5b), where it forms a submerged shoal along the margin of the Malta Horst. The anticline attains a maximum height of 145 m, and its core along the eroded culmination of the pericline is exposed at locality C (Mosta quarry), where facies association TC is exhumed (Fig. 6b, e). The Naxxar Anticline formed along a reactivated onshore segment of the Naxxar Fault that produced basin inversion of part of the Naxxar Basin. Outside the Malta Horst, the Naxxar Basin depocenter remains undeformed as seen in seismic line 1 (Fig. 3a). The angle of the upper part of the Naxxar listric fault is too steep for reactivation as a reverse fault, so a footwall shortcut (thrust 6) developed at a lower angle, which surfaces about 200 m farther west from the main fault. The thrust fault is imaged in seismic line 2 and exhumed the Lower Coralline Limestone Formation on land and offshore (Figs. 5a, b, and 6b, e).

The frontal part of the Naxxar Anticline comprises the 1.5 km-wide Wied Faham Overthrust (Fig. 7a, b) that migrated horizontally by >100 m along a low-angle (~25°) reverse fault across part of the older Great Fault (phase D). The deformed floor thrust sediments dip by 15° ESE (Fig. 7b i) and the roof thrust dips at <10° (Fig. 7b ii). The Wied Faham Overthrust developed into an overturned fold as it migrated westward along a low-angle axial plane verging NW over the ductile Blue Clay Formation (Fig. 7c), which was smeared along the floor thrust and acted as a decollement surface. The mass of the overthrust downflexed the hanging wall margin of the older Great Fault, preserving an outlier of younger rock (TG and TH) along its flank (Fig. 7b).

The dorsal part of the Naxxar Anticline hosts the Sliema-Hamrun Syncline (Fig. 5b) that doubly plunges to the SW toward Hamrun Basin and to the NE towards Sliema Syncline, separated by the Pieta Anticline (Fig. 6d, f). The Sliema end consists mostly of Lower Globigerina Limestone (TF) with a small outlier of Middle Globigerina (TG) preserved in the hangingwall of the Tigne Fault (Gatt, 2005) at locality G

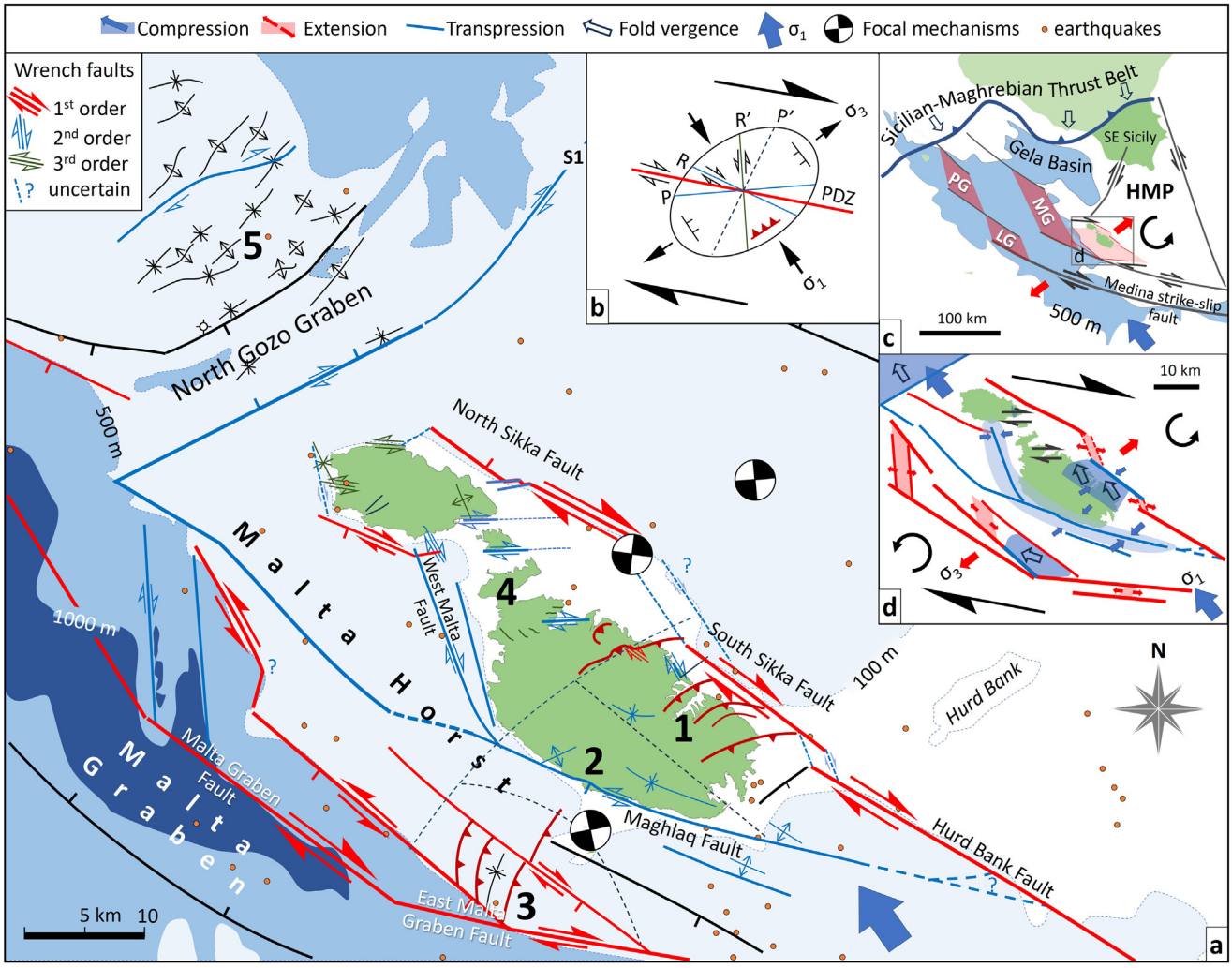

Fig. 8. Regional geodynamics and deformation by Africa-Eurasia convergence (arrows marked σ_1) (Hollenstein et al., 2003): (a) Foreland deformation of the Malta Horst: First-order master faults (122°N) that bound the Malta Horst are shown in red, second-order in blue, and third-order deformations in green. Areas 1 to 4 are based on this study and Area 5 is based on (Gardiner *et al.*, 1995). Round dots are earthquakes (data from INGV), (b) strain ellipse, (c) schematic development of the Pantelleria Rift grabens along the Medina Wrench based on (Jongsma *et al.*, 1987), and (d) compression and extension around the Maltese Islands.

(Fig. 5b). A larger outlier of the Middle Globigerina Member is preserved along the Hamrun end of the syncline over central Malta (Fig. 6a, d, and f). The Sliema and Hamrun synclines are separated by the Pieta Anticline, which is a <2 km long, imbricated in front of the larger Valletta Anticline. The Pieta Anticline interferes with the Sliema-Hamrun Syncline and exhumes the Lower Globigerina along its centre, preserving the Middle Globigerina along its flanks (Fig. 6d).

4.3 Area 2

The wedge-shaped area extends from the Great Fault on the northwest to the eastern tip of the Maghlaq Fault (M1) on the south (Fig. 3e).

Faults: Older faults formed during tectonic phase D are preserved, mostly consisting of Miocene, NE-trending faults.

Horizontal deformation:

This western part of Malta exhibits uparching of the Lower Coralline Limestone Formation, which reaches a thickness of 120 m along the cliffed coast of Malta (Fig. 5a) during tectonic phase E contraction. The deformation produced a NE-trending anticline exposed along the cliffed coast of Malta. The NW limb dips by 2° toward the NW with a lower angle dip along the SE limb. Synclines oblique to the Maghlaq Fault (M1) on land preserve a Middle Globigerina outlier along the Mqabba Basin (Figs. 5a and 6h). Most of the Malta Group sediments (TD to TK) are preserved along the western part of Area 2 (Fig. 6k), in contrast to Area 1, where sediments younger than the Aquitanian are mostly eroded.

4.4 Area 3

Area 3 consists of a 13 km wide offshore belt along the SW-facing margin of the Malta Horst that hosts the offshore

part of the Maghlaq Fault system. The area is crossed by seismic line 3 (Fig. 4b) parallel to the outer Maghlaq fault system (M4 and M5).

Faults:

The inner part of the WNW-trending Maghlaq fault system (M1) is exposed in Malta as a normal fault showing a minor sinistral slip component (Bonson *et al.*, 2007). An earthquake swarm in 2015 (Bozionelos *et al.*, 2017) between the M1 and M2 faults and older earthquakes around M3 fault suggest that they are active (Fig. 3e). The southern margin of Area 3 is bounded by the NW-trending outer Maghlaq faults (M4 and M5), which are parallel to the Malta Graben master fault. The M5 fault of the Maghlaq fault system developed as normal faults during phase D and is presently reactivated as left-lateral strike-slip faults (phase E).

Horizontal deformation:

Seismic line 3 along the SE margin of Area 3 shows uplifted Cretaceous sediments deformed by compression, capped by a relatively thin Zabbar Formation (Eocene) overlain by a series of listric faults through the Oligo-Miocene succession showing minor thrusts verging NW. The thrusts do not extend to Malta island, except for the here-named Filfla Fault and overlying anticline (Fig. 4b), which resulted in subaerial exposure of only part of the hanging wall block of the M1 Maghlaq Fault in Malta island and the tiny Filfla island (Fig. 3e). The thrusts observed in seismic imaging (line 3 in Fig. 4b) sole along the E1 gypsum bed (E-reflector). Farther west, sediments dip NW along the relay ramp between the outer Maghlaq faults (M4 and M5), which is partly filled with Plio-Quaternary sediments. Seismic line 5 shows anticlines on both sides of the M1 and M2 Maghlaq faults in offshore south Malta. These features suggest compression orthogonal to the inner Maghlaq fault system (Fig. 3e).

Area 4

Area 4 entirely overlies the West Malta Palaeohigh (WMP), which constitutes the footwall block of the Naxxar Basin (Fig. 1d). Phase E deformation in this region is characterized primarily by strike-slip kinematics and associated minor folding, largely driven by the reactivation of existing structures. The South Gozo Fault, originally characterized by 100 m of vertical displacement during the Late Miocene (phase D), now exhibits a dextral strike-slip overprint (Fig. 5d). The transcurrent movement created 250 m-wide feather structures by extension along the eastern part of the fault (Reuther, 1984), whereas compression in the western part resulted in the development of an anticline exposed along the coast. Parallel to this W–E trending fault are the South Comino strike-slip fault (Fig. 5a) and the dextral strike-slip Bugibba Fault exposed along the coast, where fault breccia from the underlying Lower Coralline Limestone Formation is exhumed along the fault with Riedel shears developing in the surrounding Lower Globigerina Limestone (TE) (Fig. 6j). En echelon strike-slip faults also formed around the southern part of the Mellieha Ridge (Fig. 5c).

The NE-trending Miocene normal faults within the North Malta Graben show evidence of reactivation and minor upthrusting (Reuther and Eisbacher, 1985), whereas the West Malta Fault (Fig. 3e), aligned with the regional compression field, functions as a strike-slip structure exhibiting transpression, which has resulted in the formation of a positive flower structure (Fig. 4d).

5 Discussion

During Phase E, NW-directed contraction reactivated pre-existing Oligo-Miocene normal faults through two distinct structural mechanisms:

- Strike-Slip Reactivation: Normal faults running parallel to the NW–SE trending margins of the Malta Horst (specifically the Sikka and Maghlaq faults) are reactivated as strike-slip faults trending sub-parallel (<30°) to the NW-directed compressional regime (σ_1). The neotectonic structures mapped in Figure 8a, show several focal mechanisms of earthquakes associated with this strike-slip type of movement (Maiorana *et al.*, 2023). These structures align to synthetic Riedel shears shown in Figure 8b, which typically constitute the first surface features to develop (Tchalenko, 1970).
- Thrust Reactivation: Normal faults trending oblique (NE–SW) or orthogonal to the horst margins (such as the Naxxar and Valletta faults) were reactivated as reverse faults. These developed into NW-verging thrusts characterized by overlying anticlines.

5.2 Regional tectonics

At the regional level, phase E contraction is consistent with the occurrence of Quaternary NW deformation in Tunisia (Bouaziz *et al.*, 2002) and the development of anticlines in the Linosa Graben and northern Malta Graben (Maiorana *et al.*, 2023; Sulli *et al.*, 2021; Civile *et al.*, 2021) and drives a right-lateral motion component of 1.7 ± 0.8 mm/yr along NW–SE striking fault systems between North Africa and Lampedusa Island (Serpelloni *et al.*, 2007).

Phase E occurs at a time of slowing down or stopping of the rollback of the Calabrian arc as shown by GPS data (Serpelloni *et al.*, 2007), accompanied by the locking of the subduction fault in the Ionian sector (Gutscher *et al.*, 2006). The end of rollback terminated foreland extension by slab-pull effect (phase D) and subjected the Pelagian foreland to the ongoing NW compression by Africa with respect to Eurasia at a rate of ~0.5 mm/yr (Nocquet, 2012; Serpelloni *et al.*, 2022) and NW–SE shortening (Palano *et al.*, 2020) as confirmed by GPS stations in southern Sicily, Malta, and the Sicily Channel that match the African plate motion (Goes *et al.*, 2004) and the NW horizontal stress and strain in the central Mediterranean region (Ragg *et al.*, 1999; Zoback, 1992).

The NW-directed compression of the rigid HMP crust induced regional strain, facilitating the displacement of structural blocks such as the Malta Horst. The dextral strike-slip movement along the Sikka Fault suggests the anticlockwise rotation of the block north of the Malta Horst and the extrusion of the Malta Horst block towards the NW, into the North Gozo Graben and Area 5, where several contractional anticlines have developed (Gardiner *et al.*, 1995) (Fig. 8a). However, the shearing and contraction of Oligo-Miocene sediments observed in Areas 1, 3, and 5 (outside the WMP) are thin-skinned features (Fig. 1d), associated with shallow-depth (<5 km) earthquakes,

whereas many earthquakes in the Malta Horst occur at a depth of about 10 km (INGV, 2025), which is close to the interface of the MICP sediments with the African granitic basement (Fig. 1d) (Gatt, 2025). At this depth, deformation is dominated by the West–East-trending PDZ.

The strain ellipse in Figure 8b shows the PDZ that developed in response to Northwest-directed stress (σ_1) within the North African craton. The PDZ developed by W–E transcurrent movement since <5 Ma that produced the dextral strike-slip movement of the Medina Wrench, which forms a 300 km long belt of transcurrent deformation along the southern boundary of the HMP microplate, which is moving eastward with respect to Africa (Jongsma *et al.*, 1987). Some authors suggest that the deep grabens within the Pantelleria Rift developed as pull-apart basins along this dextral shear zone (Boccaletti, 1987; Jongsma *et al.*, 1987; Reuther and Eisbacher, 1985) in response to transcurrent movement along the Medina Wrench (Fig. 8c). The W-E strain is manifest in the Malta Horst in two areas:

- The WNW trending eastern part of the Malta Graben Fault that is subparallel to the Medina Wrench,
- Along the W–E transcurrent faults in Area 4, which are aligned with the Medina Wrench (Fig. 8a). This alignment likely stems from the structural high of the Mesozoic WMP, which is close to the surface (Fig. 1d). Consequently, the underlying W–E thick-skinned deformation is expressed at a more advanced stage of surface emergence.

The W–E strain along these two zones frames a 50 km wide pull-apart basin encompassing the Maltese Islands, bounded on the west by the Malta Graben/Maghlaq faults and on the east by the Sikka/Hurd Bank first-order strike-slip. The fault geometry implies an active, W–E dextral transcurrent movement and diverging NE–SW strain–stress regime (σ_3), albeit with a low deformation rate (Fig. 8d).

5.3 Geometric analysis: NW–SE strike-slip faults

The right-stepping Sikka strike-slip faults produced a series of <5 km wide, W-E trending extensional oversteps that form small pull-apart basins along the margins of the Malta Horst (Fig. 8d). One of these basins is along the right-stepping South Sikka fault and Hurd Bank Fault. Extension produced the transtensional strike-slip Hurd Bank fault with a negative flower structure imaged in seismic line 5 (Fig. 4c) along its NW tip. At least two other basins are inferred from bathymetry in the hanging wall block of the outer Maghlaq fault (M5). In contrast, transpression is inferred along the South Sikka Fault from the *in situ* stress measurements (Fig. 5b). The transpression resulted in drag along the transcurrent fault, which produced the folding observed along the NE coast of Malta (Area 1).

It is suggested that the central part of the Horst Malta is under minor compression along a crescent-shaped zone that extends from the NNW-trending West Malta Fault (dextral strike-slip fault imaged along seismic line 4 in Fig. 4d) to the east part of the Maghlaq Fault imaged in seismic line 5. Both faults show positive flower structures in seismic, implying transpression, which may be accommodating extension along the conjugate margins of the Malta Horst.

5.4 NE–SW faults and folds and the E1 evaporite bed

Pre-Cenozoic contractional deformation of Mesozoic MICP sediments (Gatt, 2025) indicates a more rigid rheology compared to the younger Oligo-Miocene sequence. Because of its rigid rheology, the WMP acts as a backstop for Oligo-Miocene deformations (Fig. 1d). In regions of greater Oligo-Miocene thickness (Areas 1, 3, and 5), the resulting differential horizontal strain between the rigid Mesozoic basement and cover is resolved by strain along the E1 décollement.

The E1 gypsum bed is overlain by 20 m of argillaceous limestone, penetrated by the NAX and ZAB wells. These low shear strength beds are characterized by 50 m of breccia with large, cavernous porosity (Fig. 2a). The fracturing and caverns suggest dissolution of the gypsum bed observed in the NAX and ZAB wells (Fig. 2a) and extensive shearing along the decollement over which the Oligo-Miocene succession translated. The regional NW compression resulted in reactivation of parts of the older NE–SW trending normal faults (phase A) into thrusts that sole along the E1 gypsum bed at the Eocene-Oligocene boundary (seismic line 2). The thrusts are overlain by NW-verging folds that extend to <10 km along the NE margin of the Malta Horst (Area 1) that are exposed along the NE coast of Malta as a series of noncylindrical and doubly plunging folds. These en echelon folds developed at a 45° angle to the Sikka strike-slip faults (Fig. 5a) in the direction of shear as suggested by Sylvester (1988). The anticlines form an imbricate thrust system around the Marsascala Anticline with more isolated and increasingly asymmetrical folds farther northwest. The latter folds are associated with basement structures of the Naxxar and Valletta normal faults (tectonic phase A) that seeded thin-skinned folds and basin inversion. The well-preserved, dome-shaped Naxxar Anticline involved the reactivation of only a small section of the Naxxar Fault, which suggests that the remainder of this fault has a dip angle too steep (>60°) for reverse fault reactivation (Sibson, 1995). Nevertheless, the reactivated section developed a shortcut fault (fault 6 in Figs. 4a and 6b) in response to the steep angle of the Naxxar Fault.

In Area 1 and the eastern half of Area 2, only the Lower Globigerina Limestone and Lower Coralline Limestone formations are preserved. The Upper Coralline Limestone and Blue Clay formations were entirely removed by extensive erosion during the Phase E thrust uplift. However, outliers of Middle and Upper Globigerina members (TG and TH) and the San Leonardo Formation (TL) are preserved in the synclines (Fig. 6k). In eastern Malta, the deep erosion of the Marsascala and Zabbar anticlines indicates they are older than the Naxxar Anticline to the west. This pattern suggests that thrashing moved from east to west over time. While thrust fault tips remain buried within the older anticlines of eastern Malta, they are exhumed along the Valletta and Grand Harbour faults. In these locations, Messinian paleorivers preferentially eroded the sheared rock during glacial sea-level drawdowns, carving valleys that were subsequently submerged during Pliocene flooding (Fig. 5b).

The effect of transcurrent movement dissipates farther away from the margins of the Malta Horst so that folds observed along the margins (Areas 1 and 3) do not extend to the central part of the Malta Horst. The main deformations in the middle of the horst (Area 2) are synclines related to

transpression along the Maghlaq Fault. Thrusting with overlying anticlines is more subtle in Area 3 relative to Area 1 and affects a smaller area.

5.5 Dating of regional contraction

The Medina Wrench exhibits deformation since 5 Ma (Jongsma *et al.*, 1985) along with the development of the Pantelleria Rift (Reuther and Eisbacher, 1985), whereas N–S extension (phase D) ended at 1.5 Ma, marking the post-rift stage of the graben systems in Malta (Dart *et al.*, 1993). The early stage of phase E (<1.5 Ma) began at this time when W–E transcurrent movement along the Medina Wrench reactivated the NW-trending normal faults of the Malta Horst into strike-slip faults (Fig. 2f). The NW stress and accumulated transcurrent drag along NW-striking faults resulted in tectonic inversion of the existing NE-trending normal faults, which were reactivated as thrusts along the margins of the Malta Horst. However, the precise dating of the late stage of phase E is uncertain mainly because Quaternary sediments are mostly terrestrial and sparsely preserved except in valleys. The exception is the San Leonardo Formation (Calabrian stage) that was deposited in a shallow sea (maximum depth of 10-30 m) (Pedley, 2011) but is presently located >50 m asl. Given that the Calabrian stage eustatic highstands reached only a few meters above modern sea level (Miller *et al.*, 2005), the current elevation of the San Leonardo Formation (TL) marine sediments necessitates significant (>60 m) postdepositional tectonic uplift. This uplift was likely driven by the underlying San Leonardo thrust, which forms part of an imbricate thrust system (thrust fault 2 in Fig. 6b). The well-cemented shallow marine sediments (TL) were preserved within a synclinal structure, and with subsequent upthrusting, the soft pelagic sediments of the adjacent Zabbbar and Marsascala anticlines were truncated by erosion. Based on the Calabrian age of the San Leonardo beds proposed by Pedley (2011), upthrusting associated with the late stage of phase E began right after the Calabrian stage (<0.7 Ma), which coincides with the end of Calabrian arc rotation (van Dijk and Scheepers, 1995).

Northwest verging thrusting continued during the Holocene in the Valletta Anticline and culminates in the Naxxar Anticline. Holocene core data from Marsa (2 km from Valletta Anticline) show tectonic uplift of about 2 m since 6500 cal. BP (Carroll *et al.*, 2012), which implies uplift related to the Valletta Anticline during the mid-Holocene. Uplift of the Naxxar Anticline at the same time may have contributed to the significant increase in sediment supply in the north-flowing paleoriver of Wied il-Ghasel (Fig. 5b) recorded by Marriner *et al.* (2012), which suggests rejuvenated vertical erosion upstream related to anticline uplift.

5.6 Geohazards

Most of the larger earthquakes recorded in Malta have their epicenters in Sicily, the Sicily Channel, or Greece (Barbano *et al.*, 2021). This study shows that there are another three potential mechanisms for seismic activity much closer to the Maltese Islands: (1) The present ongoing strike-slip movement along NW-trending faults, which results in low-magnitude ($M < 4$) earthquakes very close to Malta, as happened in 2015 (Bozionelos *et al.*, 2017), and the April 2025 magnitude 3.5 earthquake at a depth of 20.8 km near the Sikka Fault (INGV, 2025) (Fig. 3e), and (2) the reactivation of <10 km-long sections of older NE–SW-trending faults along the margins of the Malta Horst (Areas 1 and 3) and the W–E transcurrent strain in Gozo (Area 4) and along the eastern Malta Graben Fault.

No recorded earthquakes are known to be directly related to the thrust faults, although the direction of horizontal compressive stress recorded in situ by Grasso *et al.* (1986) along the NE coast of Malta (Fig. 5b, c) is consistent with the NW vergence of anticlines in Area 1. The absence of known seismic activity associated with these thrust faults may be due to one of the following:

- Aseismic translation of the thrust planes along the E1 decollement,
- The NW horizontal stress becomes stored as elastic energy, which is only released when the static friction along the thrust plane is overcome, resulting in a seismic event (Doglioni, 2024). The absence of known earthquakes along the thrust planes means that the recurrence of such a seismic event is longer than the first historical record of earthquakes, which in Malta is 1542 (Galea, 2007). The long recurrence period is related to the steep angle of the thrusts.

The second mechanism is more likely as transcurrent movement along the Sikka and Maghlaq faults builds up elastic energy by drag effect along the Malta Horst margins. The deep-seated W–E transcurrent movement in Area 4 is another source of deep earthquakes linked to deformation of the basement (Fig. 1d). The overall scenario may result in a strong earthquake with epicenters very close to Malta in the future.

6 Conclusion

The Malta Horst forms the southern part of the HMP, which entered a foreland position since the Miocene. It is characterized by:

- Alternating phases of extension (phases A, B, and D) and contraction (phases C and E). The extensional phases produced successive basins: the Naxxar, Valletta, and Marsaxlokk half grabens (Oligocene-early Miocene) and the North Gozo, North Malta, and Malta grabens (Late Miocene-Pliocene).
- The change from an extensional (phase D) to the present contractional (Phase E) regime marks the slowing down of the velocity of the Calabrian arc as it migrated SE toward the North African foreland. The slowdown ended foreland extension in the HMP. The present contraction reflects the resumption of the dominance of the ongoing convergence of Africa towards Eurasia since the Late Cretaceous.
- The present contractional phase E reactivated the Late Miocene to Pliocene NW-trending normal faults (phase D) parallel to the margins of the Malta Horst by dextral transcurrent movement to accommodate the compression.
- The NW compressive event reactivated the NE-trending Oligo-Miocene faults into thrusts and inverted half-grabens of phase A into a series of NW-verging anticlines and synclines oblique to the margins of the Malta Horst (Areas 1 and 3). The Oligo-Miocene sediments underwent

thin-skinned contraction facilitated by late Eocene to early Oligocene evaporite and marly beds acting as a decollement surface.
– The underlying Mesozoic basement (West Malta Palaeohigh) acted as a backstop to thin-skinned thrusting. Deformation in Area 4 (WMP) is along W-E strike-slip faults and reflects the regional PDZ from NW compression.
– Present compression is pushing the Malta Horst towards the NW into Area 5, where thin-skinned deformation by folding is common.
– The compressive structures in Malta are still active, although not associated with historical seismic events, which suggests either slow ductile deformation along evaporite décollements or a long recurrence period of seismic events.

Acknowledgments

BP and Total are thanked for providing well data and TGS for the seismic sections. I thank the editor Prof. Juan Soto for his comments on the text and encouragement as well as two other anonymous reviewers. This study is partly based on the author's PhD thesis at the University of Durham, UK.

References

Argnani A. 1987. Gela nappe: evidence of accretionary melange in the Maghrebian foredeep of Sicily. *Mem Soc Geol It* 38: 419–428.
Argnani A. 1990. The Strait of Sicily rift zone: foreland deformation related to the evolution of a back-arc basin. *J Geodyn.* 12: 311–331.
Baldassini N, Di Stefano A. 2017. Stratigraphic features of the Maltese Archipelago: a synthesis. *Nat Hazards* 86: 203–231. https://doi.org/10.1007/s11069-016-2334-9
Bally AW. 1984. Tectogenese et sismique reflexion. *Bull Soc Géol France* S7-XXVI(2): 279–285. https://doi.org/10.2113/gssgfbull.S7-XXVI.2.279
Barbano MS, Castelli V, Galea P, Pirrotta C. 2021. Materials for a seismic history of the Maltese Islands. *Quad Geofis* 171: 1–358. https://doi.org/10.13127/qdg/171
Ben-Avraham Z, Lyakhovsky V, Grasso M. 1995. Simulation of collision zone segmentation in the central Mediterranean. *Tectonophysics* 243(1–2): 57–68. https://doi.org/10.1016/0040-1951(94)00191-B
Bialik OM, Zammit R, Micallef A. 2021. Architecture and sequence stratigraphy of the Upper Coralline Limestone formation, Malta—implications for Eastern Mediterranean restriction prior to the Messinian Salinity Crisis. *Depos Rec* 7(2): 256–270. https://doi.org/10.1002/dep2.138
Boccaletti M. 1987. Transtensional tectonics in the Sicily Channel. *J Struct Geol* 9(7).
Bonini M, Sani F, Antonielli B. 2012. Basin inversion and contractional reactivation of inherited normal faults: a review based on previous and new experimental models. *Tectonophysics* 522–523: 55–88. https://doi.org/10.1016/j.tecto.2011.11.014
Bonson CG, Childs C, Walsh JJ, Schöpfer MPJ, Carboni V. 2007. Geometric and kinematic controls on the internal structure of a large normal fault in massive limestones: the Maghlaq Fault, Malta. *J Struct Geol* 29(2): 336–354. https://doi.org/10.1016/j.jsg.2006.06.016
Bouaziz S, Barrier E, Soussi M, Turki MM, Zouari H. 2002. Tectonic evolution of the northern African margin in Tunisia from paleostress data and sedimentary record. *Tectonophysics* 357: 227–253.
Bozionelos G, Galea P, D'Amico S, Agius M. 2017. Characteristics of the recent seismic activity on a near-shore fault south of Malta, Central Mediterranean. *Geophys Res Abstr EGU* 19: 2017–17929.
Burgess PM, Winefield P, Minzoni M, Elders C. 2013. Methods for identification of isolated carbonate buildups from seismic reflection data. *AAPG Bulletin* 97(7): 1071–1098. https://doi.org/10.1306/12051212011
Butler R.W.H, Grasso M, La Manna F. 1992. Origin and deformation of the Neogene-Recent Maghrebian foredeep at the Gela Nappe, SE Sicily. *J Geol Soc* 149: 547–556.
Butler R.W.H, Bond C.E, Robledo F. 2025. Basement Controls on Structural Evolution in Thin-Skinned Thrust Belts—Implications for Migration of Deformation Into Orogenic Forelands. *Tect* 44(1). https://doi.org/10.1029/2024TC008347
Cahuzac B, Poignant A. 1997. Essai de biozonation de l'Oligo-Miocene dans les bassins europeen a l'aide des grands foraminiferes neritique. *Bull. Soc. Geol. France*, 168(2): 155–169.
Carroll FA, Hunt CO, Schembri PJ, Bonanno A. 2012. Holocene climate change, vegetation history and human impact in the Central Mediterranean: evidence from the Maltese Islands. *Quat Sci Rev* 52: 24–40. https://doi.org/10.1016/j.quascirev.2012.07.010
Ciarcia S, Vitale S. 2024. Orogenic evolution of the northern Calabria−southern Apennines system in the framework of the Alpine chains in the central-western Mediterranean area. *Geol Soc Am Bull*. https://doi.org/10.1130/B37474.1
Civile D, Brancolini G, Lodolo E, Forlin E, Accaino F, Zecchin M, Brancatelli G. 2021. Morphostructural setting and tectonic evolution of the central part of the Sicilian Channel (Central Mediterranean). *Lithosphere* 2021(1): 1–24. https://doi.org/10.2113/2021/7866771
Cogan J, Rigo L, Grasso M, Lerche I. 1989. Flexural tectonics of southeastern Sicily. *J Geodyn* 11(3): 189–241. https://doi.org/10.1016/0264-3707(89)90007-0
Corti G, Cuffaro M, Doglioni C, Innocenti F, Manetti P. 2006. Coexisting geodynamic processes in the Sicily Channel. *Geol Soc Am Spec Pap* 409: 83–96. https://doi.org/10.1130/2006.2409(05)
Cowie L, Kusznir N. 2012. Mapping crustal thickness and oceanic lithosphere distribution in the Eastern Mediterranean using gravity inversion. *Pet Geosci* 18(4): 373–380. https://doi.org/10.1144/petgeo2011-071
Dart CJ, Bosence DW, McClay KR. 1993. Stratigraphy and structure of the Maltese graben system. *J Geol Soc London* 150: 1153–1166.
Decelles PG, Giles KA. 1996. Foreland basin systems. *Basin Res* 8: 105–123.
Dewey J, Pitman W.C, Ryan W, Bonin J. 1973. Plate tectonics and the evolution of the Alpine system. *Geol Soc Amer Bull* 84: 3137–180.
Dewey JF, Helman ML, Knott SD, Turco E, Hutton DHW. 1989. Kinematics of the western Mediterranean. *Geol Soc Spec Publ* 45: 265–283. https://doi.org/10.1144/GSL.SP.1989.045.01.15
Doglioni C. 2024. Gravitational and elastic energies stored in crustal volumes activate normal versus strike-slip and thrust seismogenic faults. *Geosci Front* 15(6): 101894. https://doi.org/10.1016/j.gsf.2024.101894
Dunham RJ. 1962. Classification of carbonate rocks according to depositional texture. In: Ham WE, ed. *Classification of carbonate rocks—A Symposium*, pp. 108–121.
Embry AF, Klovan JE. 1971. A Late Devonian reef tract on northeastern Banks Island, Northwest Territories. *Bull. Can. Petrol. Geol.*, 58: 730–781.

Faccenna C, Piromallo C, Crespo-Blanc A, Jolivet L, Rossetti F. 2004. Lateral slab deformation and the origin of the western Mediterranean arcs. *Tectonics 23*(1). https://doi.org/10.1029/2002TC001488

Felix R. 1973. *Oligo-Miocene stratigraphy of Malta and Gozo*, Vols 73–20. Veeman Zonen.

Finetti I. 1982. Structure, stratigraphy and evolution of the Central Mediterranean. *Boll Geof Teor Appl* XXIV(96): 247–312.

Galea P. 2007. Seismic history of the Maltese Islands and considerations on seismic risk. *Ann Geophys* 50: 725–740.

Gallais F, Gutscher MA, Graindorge D, Chamot-Rooke N, Klaeschen D. 2011. A Miocene tectonic inversion in the Ionian Sea (central Mediterranean): evidence from multichannel seismic data. *J Geophys Res Solid Earth* 116(12). https://doi.org/10.1029/2011JB008505

Gardiner W, Grasso M, Sedgeley D. 1995. Plio-Pleistocene fault movement as evidence for mega-block kinematics within the Hyblean-Malta Plateau, Central Mediterranean. *J Geodyn* 19 (1): 5–51.

Gatt P. 2005. Syntectonic deposition of an Oligo-Miocene phosphorite conglomerate bed in Malta. *Centr Mediterr Nat* 4(2): 109–118.

Gatt P. 2007. Controls on Plio-Quaternary foreland sedimentation in the region of the Maltese Islands. *Boll Soc Geol Ital* 126(1): 119–129.

Gatt P. 2012. *Carbonate facies, depositional sequences and tectonostratigraphy of the Paleogene Malta Platform*. Unpublished PhD thesis, University of Durham, UK. https://etheses.dur.ac.uk/4425/

Gatt P. 2019. Evaporite dissolution sinkholes in the Dwejra Depression, Malta. *Eur Geol* 48: 53–57.

Gatt P. 2022. Facies, depositional environments and drowning of Tethyan isolated carbonate platforms: the Paleogene carbonates of Malta. *Facies* 68(3): 9. https://doi.org/10.1007/s10347-022-00648-1

Gatt P. 2025. Tectonic segmentation of the Mesozoic to Paleogene Malta Isolated Carbonate Platform: a key to rifting in the Central Mediterranean. *Tectonics* 44: e2025TC008902. https://doi.org/10.1029/2025TC008902

Gatt PA. 2006. Model of limestone weathering and damage in masonry: Sedimentological and geotechnical controls in the Globigerina Limestone Formation (Miocene) of Malta. *Xjenza* 11: 30–39.

Gatt P, Tucker M, Davies R. 2009. Drowning of the Malta carbonate platform: facies and sequence stratigraphy of the Lower Coralline Limestone (U. Oligocene). In: Pascucci V, Andreucci S, eds. *Sedimentary environments of Mediterranean islands*. International Association of Sedimentologists, p. 181.

Goes S, Jenny S, Hollenstein C, Kahle HG, Geiger A. 2004. A recent tectonic reorganization in the south-central Mediterranean. *Earth Planet Sci Lett* 226(3–4): 335–345. https://doi.org/10.1016/j.epsl.2004.07.038

Grasso M, Pedley HM. 1985. The Pelagian Islands: A new geological interpretation from sedimentological and tectonic studies and its bearing on the evolution of the Central Mediterranean (Pelagian block). *Geologica Rom.* 24: 13–34.

Grasso M, Reuther C-D, Baumann H, Becker A. 1986. Shallow crustal stress and neotectonic framework of the Malta platform and the southeastern Pantelleria Rift (Central Mediterranean). *Geologica Rom* 25: 191–212.

Guiraud R, Bosworth W. 1999. Phanerozoic geodynamic evolution of northeastern Africa and the northwestern Arabian platform. In: *Tectonophysics*, Vol. 315. www.elsevier.com/locate/tecto

Gutscher MA, Kopp H, Krastel S, Bohrmann G, Garlan T, Zaragosi S, *et al.* 2017. Active tectonics of the Calabrian subduction revealed by new multi-beam bathymetric data and high-resolution seismic profiles in the Ionian Sea (Central Mediterranean). *Earth Planet Sci Lett* 461: 61–72. https://doi.org/10.1016/j.epsl.2016.12.020

Gutscher MA, Roger J, Baptista MA, Miranda JM, Tinti S. 2006. Source of the 1693 Catania earthquake and tsunami (southern Italy): new evidence from tsunami modeling of a locked subduction fault plane. *Geophys Res Lett* 33(8). https://doi.org/10.1029/2005GL025442

Harrison JC. 1954. Gravity measurement on Malta and Tunis. *Geophys J Int* 6: 604–609. https://doi.org/10.1111/j.1365-246X.1954.tb03043.x

Hilgen FJ, Abels HA, Iaccarino S, Krijgsman W, Raffi I, Sprovieri R, *et al.* 2009. The Global Stratotype Section and Point (GSSP) of the Serravallian Stage (Middle Miocene). *Episodes* 32(3): 152–166. https://doi.org/10.18814/epiiugs/2009/v32i3/002

Hollenstein Ch, Kahle H-G, Geiger A, Jenny S, Goes S, Giardini D. 2003. New GPS constraints on the Africa-Eurasia plate boundary zone in southern Italy. *Geophys Res Lett* 30(18). https://doi.org/10.1029/2003GL017554

Hsu K, Ryan W, Cita M. 1973. Late Miocene dessication of the Mediterranean. *Nature* 242: 240–244.

Illies JH. 1981. Graben formation—the Maltese Islands, a case history. *Tectonophysics* 73: 151–168.

INGV. 2025. https://terremoti.ingv.it/en

Jolivet L, Faccenna C. 2000. Mediterranean extension and the Africa-Eurasia collision. *Tectonics* 19(6): 1095–1106. https://doi.org/10.1029/2000TC900018

Jongsma D, van Hinte JE, Woodside JM. 1985. Geologic structure and neotectonics of the North African continental margin south of Sicily. *Mar Pet Geol* 2(2): 156–179. https://doi.org/10.1016/0264-8172(85)90005-4

Jongsma D, Woodside JM, King GCP, Van Hinte JE. 1987. The Medina Wrench: a key to the kinematics of the central and eastern Mediterranean over the past 5 Ma. *Earth Planet Sci Lett* 82: 87–106.

Krijgsman W, Hilgen FJ, Raffi I, Sierro FJ, Wilson DS. 1999. Chronology, causes and progression of the Messinian salinity crisis. *Nature* 400: 652–655. www.nature.com

Letouzey J, Colletta B, Chermette JC. 1995. Evolution of Salt-Related Structures in Compressional Settings. In: Jackson M, Roberts DG, Snelson S, eds. *Salt Tectonics: A Global Perspective*. pp. 41–60. AAPG Memoir 65. https://archives.datapages.com/data/specpubs/memoir65/ch03/0041.htm

Maiorana M, Artoni A, Le Breton E, Sulli A, Chizzini N, Torelli L. 2023. Is the Sicily Channel a simple Rifting Zone? New evidence from seismic analysis with geodynamic implications. *Tectonophysics* 864. https://doi.org/10.1016/j.tecto.2023.230019

Malinverno A, Ryan WBF. 1986. Extension in the Tyrrhenian Sea and shortening in the Apennines as result of arc migration driven by sinking of the lithosphere. *Tectonics* 5(2). https://doi.org/10.1029/TC005i002p00227

Marriner N, Gambin T, Djamali M, Morhange C, Spiteri M. 2012. Geoarchaeology of the Burmarrad ria and early Holocene human impacts in western Malta. *Palaeogeogr Palaeoclimatol Palaeoecol* 339–341: 52–65. https://doi.org/10.1016/j.palaeo.2012.04.022

Martinelli M, Bistacchi A, Balsamo F, Meda M. 2019. Late Oligocene to Pliocene extension in the Maltese Islands and implications for geodynamics of the Pantelleria Rift and Pelagian Platform. *Tectonics* 38(9): 3394–3415. https://doi.org/10.1029/2019TC005627

Miller KG, Browning JV, Schmelz WJ, Kopp RE, Mountain GS, Wright JD. 2020. Cenozoic sea-level and cryospheric evolution from deep-sea geochemical and continental margin records. *Sci Adv* 6(20): eaaz1346. https://www.science.org

Miller KG, Kominz MA, Browning JV, Wright JD, Mountain GS, Katz ME, et al. 2005. The phanerozoic record of global sea-level change. *Science* 310: 1293–1298. https://doi.org/10.1126/science.1116412

Moody JD, Hill MJ. 1956. Wrench-fault tectonics. *Geol Soc Am Bull* 67(9): 1207–1246. https://doi.org/10.1130/0016-7606(1956)67[1207:WT]2.0.CO;2

Morticelli M.G, Valenti V, Catalano R, Sulli A, Agate M, Avellone G, Albanese C, Basilone L, & Gugliotta C. 2015. Deep controls on foreland basin system evolution along the Sicilian fold and thrust belt. *Bull Soc Géol France* 186(5): 4–5.

Nocquet J-M. 2012. Present-day kinematics of the Mediterranean: A comprehensive overview of GPS results. *Tectonophysics* 579: 220–242. https://doi.org/10.1016/j.tecto.2012.03.037

Palano M, Ursino A, Spampinato S, Sparacino F, Polonia A, Gasperini L. 2020. Crustal deformation, active tectonics and seismic potential in the Sicily Channel (Central Mediterranean), along the Nubia–Eurasia plate boundary. *Sci Rep* 10(1). https://doi.org/10.1038/s41598-020-78063-1

Pedley HM. 1978. A new lithostratigraphical and palaeoenvironmental interpretation for the coralline limestone formations (Miocene) of the Maltese Islands. *Overseas Geol Miner Resour* 54: 1–17. https://pubs.bgs.ac.uk/publications.html?pubID=B03990#f=true&v=d&z=2&n=5&i=B03990_0011.jp2&y=750&x=306

Pedley HM, Grasso M. 1992. Miocene syntectonic sedimentation along the western margins of the Hyblean-Malta platform: a guide to plate margin processes in the central Mediterranean. *J Geodyn* 15 (1): 19–37.

Pedley HM, House MR, Waugh B. 1976. The geology of Malta and Gozo. *Proc Geol Assoc* 87(3): 325–341. https://doi.org/10.1016/S0016-7878(76)80005-3

Pedley HM, House MR, Waugh B. 1978. The geology of the Pelagian Block: the Maltese Islands. In: Nairn AEM, Kanes WH, Stehli FG, eds. *The Ocean Basins and margins.* Plenum Press, pp. 417–433.

Pedley M. 2011. The Calabrian stage, Pleistocene highstand in Malta: a new marker for unravelling the Late Neogene and Quaternary history of the islands. *J Geol Soc* 168(4): 913–926. https://doi.org/10.1144/0016-76492010-080

Putz-Perrier MW, Sanderson DJ. 2010. Distribution of faults and extensional strain in fractured carbonates of the North Malta Graben. *Am Assoc Pet Geol Bull* 94(4): 435–456. https://doi.org/10.1306/08260909063

Ragg S, Grasso M, Müller B. 1999. Patterns of tectonic stress in Sicily from borehole breakout observations and finite element modeling. *Tectonics* 18(4): 669–685. https://doi.org/10.1029/1999TC900010

Reuther CD. 1984. Tectonics of the Maltese Islands. *Centro* 1: 1–20.

Reuther C-D, Eisbacher GH. 1985. Pantelleria Rift-crustal extension in a convergent intraplate setting. *Geolog Rundsch* 74(3): 585–597.

Ricou LE. 1994. La thétys reconstruite: plaques, blocs continentaux et leurs limites depuis 260 ma de l'amérique centrale à l'asie du sud-est. *Geodinam Acta* 7(4): 169–218. https://doi.org/10.1080/09853111.1994.11105266

Rosenbaum G. 2014. Geodynamics of oroclinal bending: Insights from the Mediterranean. *J Geodyn* 82: 5–15. https://doi.org/10.1016/j.jog.2014.05.002

Rosenbaum G, Lister GS, Duboz C. 2002. Relative motions of Africa, Iberia and Europe during Alpine orogeny. *Tectonophysics* 359: 117–129. www.elsevier.com/locate/tecto

Rosenbaum G, Lister G. 2004. Formation of arcuate orogenic belts in the western Mediterranean region. In A. J. Sussman A. B. Weil (Eds.), Formation of arcuate orogenic belts in the western Mediterranean region (pp. 41–56). *Geol. Soc. Am. Spec. Pap* 383.

Roure F, Casero P, Addoum B. 2012. Alpine inversion of the North African margin and delamination of its continental lithosphere. *Tectonics* 31(3). https://doi.org/10.1029/2011TC002989

Roveri M, Flecker R, Krijgsman W, Lofi J, Lugli S, Manzi V, *et al.* 2014. The Messinian Salinity Crisis: Past and future of a great challenge for marine sciences. *Marine Geol* 352: 25–58. https://doi.org/10.1016/j.margeo.2014.02.002

Rusciadelli G, Shiner P. 2018. Isolated carbonate platforms of the Mediterranean and their seismic expression—searching for a paradigm. *Lead Edge* 37(7): 492–501. https://doi.org/10.1190/tle37070492.1

Serpelloni E, Cavaliere A, Martelli L, Pintori F, Anderlini L, Borghi A, *et al.* 2022. Surface velocities and strain-rates in the Euro-Mediterranean region from massive GPS data processing. *Front Earth Sci* 10. https://doi.org/10.3389/feart.2022.907897

Serpelloni E, Vannucci G, Pondrelli S, Argnani A, Casula G, Anzidei M, *et al.* 2007. Kinematics of the Western Africa-Eurasia plate boundary from focal mechanisms and GPS data. *Geophys J Int* 169(3): 1180–1200. https://doi.org/10.1111/j.1365-246X.2007.03367.x

Serra-Kiel J, Hottinger L, Esmeralda C, Drobne K, Ferrandez C, Jauhri AJ, *et al.* 1998. Larger formainiferal biostratigraphy of the Tethyan Paleocene and Eocene. *Bull Soc Geol France* 169(2): 281–299.

Sibson RH. 1995. Selective fault reactivation during basin inversion: Potential for fluid redistribution through fault-valve action. *Geolog Soc Spec Publ* 88: 3–19. https://doi.org/10.1144/GSL.SP.1995.088.01.02

Soumaya A, Ben Ayed N, Delvaux D, Ghanmi M. 2015. Spatial variation of present-day stress field and tectonic regime in Tunisia and surroundings from formal inversion of focal mechanisms: geodynamic implications for central Mediterranean. *Tectonics* 34 (6): 1154–1180. https://doi.org/10.1002/2015TC003895

Speranza F, Hernandez-Moreno C, Avellone G, Gasparo Morticelli M, Agate M, Sulli A, *et al.* 2018. Understanding Paleomagnetic Rotations in Sicily: Thrust Versus Strike-Slip Tectonics. *Tectonics* 37(4): 1138–1158. https://doi.org/10.1002/2017TC004815

Speranza F, Minelli L, Pignatelli A, Chiappini M. 2012. The Ionian Sea: The oldest in situ ocean fragment of the world? *J Geophy Res Solid Earth* 117(12). https://doi.org/10.1029/2012JB009475

Sulli A, Gasparo Morticelli M, Agate M, Zizzo E. 2021. Active north-vergent thrusting in the northern Sicily continental margin in the frame of the quaternary evolution of the Sicilian collisional system. *Tectonophysics* 802: 228717. https://doi.org/10.1016/j.tecto.2021.228717

Sylvester A. 1988. Strike-slip faults. *Bull Geol Soc America* 100(11): 1666–1703. https://doi.org/10.1130/0016-7606(1988)100<1666:SSF>2.3.CO;2

Tchalenko JS. 1970. Similarities between shear zones of different magnitudes. *Bull Geol Soc America* 81(6): 1625–1640. https://doi.org/10.1130/0016-7606(1970)81[1625:SBSZOD]2.0.CO;2

Tugend J, Chamot-Rooke N, Arsenikos S, Blanpied C, Frizon de Lamotte D. 2019. Geology of the Ionian Basin and margins: a key to the East Mediterranean geodynamics. *Tectonics* 38(8): 2668–2702. https://doi.org/10.1029/2018TC005472

van Dijk JP, Scheepers PJJ. 1995. Neotectonic rotations in the Calabrian Arc; implications for a Pliocene-Recent geodynamic scenario for the Central Mediterranean. *Earth Sci Rev* 39: 207–246.

van Hinsbergen DJJ, Torsvik TH, Schmid SM, Maţenco LC, Maffione M, Vissers RLM, *et al.* 2020. Orogenic architecture of the Mediterranean region and kinematic reconstruction of its tectonic evolution since the Triassic. *Gondwana Res* 81: 79–229. https://doi.org/10.1016/j.gr.2019.07.009

Vossmerbaumer H. 1972. *Malta: ein Beitrag zur Geologie und Geomorphologie des Zentral-Mediterranean Raumes*. Wurzburger Geographisce Arbeiten 38.

Wardell Armstrong. 1996. *Mineral Resources Assessment for the Planning Authority of Malta*.

Zoback ML. 1992. First- and second-order patterns of stress in the lithosphere: the world stress map project. *J Geophy Res* 97: 11703–11728. https://digitalcommons.unl.edu/usgsstaffpub/461

Zwaan F, Schreurs G, Buiter SJH, Ferrer O, Reitano R, Rudolf M, *et al.* 2022. Analogue modelling of basin inversion: a review and future perspectives. *Solid Earth* 13(12): 1859–1905. https://doi.org/10.5194/se-13-1859-2022

Cite this article as: Gatt P. 2026. Neotectonic shortening and foreland structural evolution of the Malta Horst Cenozoic carbonate succession, Central Mediterranean, *BSGF - Earth Sciences Bulletin* 197: 11. https://doi.org/10.1051/bsgf/2026002